COMPARISON OF MODIS AND VIIRS SNOW COVER PRODUCTS FOR THE 2016 HYDROLOGICAL YEAR

A Thesis

by

SHUBHECHCHHA THAPA

Submitted to the Office of Graduate and Professional Studies of
Texas A&M University
in partial fulfillment of the requirements for the degree of

MASTER OF SCIENCE

Chair of Committee,	Andrew G. Klein
Committee Members,	Anthony M. Filippi
	Sorin C. Popescu
Head of Department,	David M. Cairns

December 2017

Major Subject: Geography

ABSTRACT

The VIIRS (Visible Infrared Imaging Radiometer Suite) on board the Suomi-NPP (National Polar-orbiting Partnership) satellite aims to provide long-term continuity of several environmental data series including snow cover initiated with the MODIS (Moderate Resolution Imaging Spectroradiometer) instrument carried aboard Aqua and Terra satellites. There are speculations concerning differences between MODIS and VIIRS snow cover products because of different spatial resolution and spectral coverage. However, the quantitative comparisons between VIIRS and MODIS snow products are currently limited. Consequently, this study intercompares MODIS and VIIRS snow products during the 2016 hydrological year. To accomplish its research objectives, 244 swath snow products from MODIS/Aqua (MYD10L2) and the VIIRS EDR (VSCMO/binary) were intercompared for the 2016 hydrological year from October 1, 2015 to May 31, 2016 using confusion matrices, comparison maps and false color imagery.

The current VIIRS snow product is binary, therefore to produce MODIS binary snow maps, the MODIS snow cover fraction threshold value of 30% was determined by examining snow cover area at four different thresholds (20%, 30%, 40% and 50%) and comparing them with the VIIRS binary snow map. Overall VIIRS appears to map more snow and less clouds than MODIS. On average, MODIS snow maps mapped snow but VIIRS in 1% of cloud free pixels, whereas 2% of the time VIIRS mapped snow but MODIS did not. The average agreement between MODIS and VIIRS was approximately

98% indicating good agreement between them. Agreement between MODIS and VIIRS was high during the winter but lower during late fall and spring, mostly over dense forest. Both MODIS and VIIRS often mapped snow/no-snow transition zones as cloud. The visual comparison depicts good qualitative agreement between snow cover area visible in MODIS and VIIRS false color imagery and mapped in their respective snow cover products.

DEDICATION

This thesis is dedicated to my beloved mother, Mithu Thapa.

ACKNOWLEDGEMENTS

Firstly, I would like to express my sincere gratitude to my advisor, Dr. Klein for his continuous support and guidance throughout the course of this research. Besides my advisor, I would like to thank the rest of my committee members, Dr. Filippi and Dr. Popescu for their support and encouragement in this research.

My sincere thanks also go to Texas A&M University Geography department faculty, staffs and friends for making my time at Texas A&M University a great experience. I would particularly like to thank Yolanda McDonald and Swetha Peteru for their support, encouragements and wonderful company throughout my time in aggieland.

Finally, I would like to thank my parents (Mithu Thapa and Kham Bahadur Thapa), my husband (Parveen Kumar Chhetri), my aunts (Sabitri Thapa and Jenisha Thapa), my in-laws (Chakra Bahadur Chhetri, Jiwan Chhetri and Purnima Chhetri), my brothers (Subhash Thapa and Sushil Thapa) and my sister (Sadichchha Thapa) for their love, support and encouragement throughout my years of study.

CONTRIBUTORS AND FUNDING SOURCES

This work was supervised by a thesis committee consisting of Professor Andrew Klein and Professor Anthony Filippi of the Department of Geography and Professor Sorin Popescu of the Department of Ecosystem Science and Management. All work for the thesis was completed independently by the student.

My graduate study was supported by a graduate assistantship from the Department of Geography, Texas A&M University and an International Fellowship from the Association of American University Women (AAUW).

NOMENCLATURE

ATBD	Algorithm Theoretical Basis Document
AVHRR	Advanced Very High Resolution Radiometer
BRDF	Bi-directional Reflectance Distribution Function
CDR	Climate Data Record
CLASS	Comprehensive Large Array-data Stewardship System
EDR	Environmental Data Records
EOS	Earth Observing Satellite
FSC	Fractional Snow Cover
HDF	Hierarchical Data Format
IDPS EDR	Interface Data Processing Segment Environmental Data Records
IP	Intermediate Product
JPSS	Joint Polar Satellite System
LAADS	Level 1 and Atmospheric Archive and Distribution System
LANCE	Land Atmosphere Near-real-time Capability
LPV	Land Product Validation
MODIS	Moderate Resolution Imaging Spectroradiometer
MSS	Multispectral Scanner System
NASA	National Aeronautics and Space Administration
NCEP	National Centers for Environmental Prediction
NDSI	Normalized Difference Snow Index

NESDIS	National Environmental Satellite, Data and Information Service
NIST	National Institute of Standards and Technology
NOAA	National Oceanic and Atmospheric Administration
NPP	NPOESS Preparatory Project
NWS	National Weather Service
PEATE	Product Evaluation and Test Element
POES	Polar Operational Environmental Satellites
QF	Quality Flag
RDR	Raw Data Records
SCA	Snow Cover Area
SCE	Snow Cover Extent
SDR	Sensor Data Records
S-NPP	Suomi National Polar-Orbiting Partnership
SWIR	Short Wave Infrared
TEM	Thermal Emissive Bands
TM	Thematic Mapper
UFOV	Unobstructed Field of View
VCM	VIIRS Cloud Mask
VIIRS	Visible Infrared Imaging Radiometer Suite
VNIR	Visible and Near-Infrared

TABLE OF CONTENTS

Page

LIST OF FIGURES

Page

LIST OF TABLES

Page

1. INTRODUCTION

1.1 Importance of Snow Cover

Snow plays significant role in the Earth surface energy balance and affects climate at local, regional and global scales (Vikhamar and Solberg, 2002). Snow cover directly controls the Earth radiation budget as snow has very high albedo, reflecting 80 to 90 percent of the incoming solar radiation (Edwards et al., 2007; Deng et al., 2015). Seasonal snow greatly influences the hydrological cycles since snowmelt is the key source of river runoff and ground water recharge, particularly the middle and high latitudes (Solberg and Andersen, 1994; Vikhamar and Solberg, 2002; Edwards et al., 2007). Moreover, seasonal snow is the major source of hydroelectric power generation, particularly in areas where more than 50% of precipitation is in the form of snow (Solberg and Andersen, 1994; Vikhamar and Solberg, 2002).

Snow cover extent is one of the most useful indicators of climate condition (Leathers and Luff, 1997; Ault et al., 2006; Key et al., 2013). Precise monitoring and mapping of snow cover extent is critical for understanding climate change, climate dynamics and hydrological phenomena. The information on spatial extent and distribution of snow cover is an important input factor for climate and hydrological modelling (Solberg and Andersen 1994; Rosenthal and Dozier 1996; Vikhamar and Solberg 2002; Salomonson and Appel 2004), weather forecasting (Romanov, 2015), determining Earth radiation budget (Dozier, 1989), estimating snowmelt runoff for water resource management and hydropower production (Butt and Bilal, 2011; Dietz et al.,

2012), and for modelling flood hazard potential from snowmelt (Maurer et al., 2003, Huang et al., 2011). Moreover, snow cover information is used in monitoring snow cover extent and duration, validating the hydrological models, and in developing environmental data records (Dobreva and Klein, 2011; Riggs et al., 2016a).

1.2 Satellite Snow Cover Mapping

Satellite remote sensing allows for the detection and mapping of snow cover extent (SCE) at regional and global scales, and has a potential for extending local *in situ* snow measurements (Ault et al., 2006). Satellite remote sensing also offers consistent snow cover observation over large and remote areas, which can be used in long term environmental studies (Dobreva and Klein, 2011). Satellite snow cover mapping was initiated when TIROS-1 (Television and InfraRed Observation Satellite) captured the first snow cover image of Eastern Canada in April 1, 1960 (Lucas and Harrison, 1990; Deng et al., 2015). In mid-1960s, weekly snow maps at 3.7 km spatial resolution were produced following the launch of the Environmental Science Service Administration (ESSA) satellite in 1965. In 1966, National Oceanic and Atmospheric Administration (NOAA) began to produce weekly snow cover maps from polar-orbiting and geostationary satellites and surface observations (Baker, 2011; Salomonson and Appel, 2004). However, the revolution of satellite snow cover mapping started with launch of first Landsat satellite (Landsat-1) in 1972 that offered basin scale snow cover mapping at 60 m spatial resolution (Solberg and Andersen, 1994; 2006). In 1982, short wave infrared (SWIR) band of Landsat-4 TM allowed for the snow/cloud discrimination and

snow cover mapping at 30 m spatial resolution (Dozier, 1989). Since then, regional and global snow cover maps have been developed using satellite data from Geostationary Operational Environmental Satellite (GEOS), AVHRR, Landsat, Airborne Visible/Infrared Imaging Spectrometer (AVIRIS) (Lucas and Harrison, 1990; Huang et al., 2011), and most significantly from the Moderate Resolution Imaging Spectroradiometer (MODIS).

The MODIS on board Terra (EOS-AM1) and Aqua (EOS-PM1) is a multispectral instrument that provides global daily coverage data in 36 spectral bands ranging from 0.405 μm to 14.385 μm at various spatial resolutions (2 bands at 250 m, 5 bands at 500 m and 29 bands at 1 km) (Klein and Barnett, 2003; Salomonson and Appel, 2004). Terra and Aqua are the sun-synchronous multi-national NASA scientific research satellites that revolve around the Earth, carrying five remote sensing instruments including the MODIS. The Terra was launched on December 18, 1999 and provided data from February 24, 2000 to present while the Aqua was launched on May 4, 2002 and provided data from June 24, 2002 to present. Since 2000, MODIS has greatly contributed to the historical record of snow cover extent by providing moderate resolution (500 m) snow cover products ranging from 5-minute swath products, daily products to monthly SCE products.

Furthermore, Visible Infrared Imaging Radiometer Suite (VIIRS) on board Suomi-National Polar-orbiting Partnership (NPP) satellite and future Joint Polar Satellite System (JPSS) satellite was launched on October 28, 2011 with a critical role of providing long-term observations of the earth surface (Justice et al., 2013; Riggs et al.,

2016b). The VIIRS is a scanning radiometer that provides global daily coverage data in 22 spectral bands ranging from 0.412 μm to 12.01 μm at various spatial resolution, which includes 16 moderate resolution bands (M-bands) with 750 m spatial resolution, 5 spectral bands (I-bands) centered at visible, near infrared, shortwave infrared, middle infrared and far infrared spectral range at 375 m spatial resolution, and one panchromatic day/night band (DNB) with a 750 m spatial resolution (Riggs et al., 2016b). The VIIRS swath area is about 3040 km by 570 km and completes the Earth's surface coverage at least twice a day (Romanov, 2015). The VIIRS instrument represents the extension of the MODIS and AVHRR sensors (Zhang et al., 2016).

Through the launch of VIIRS, there is a potential for the augmentation of historical snow cover data records with greater precision at 375 m spatial resolution. The VIIRS snow cover products should have comparable accuracy with the MODIS snow cover products and shall provide long-term continuity of MODIS snow cover products. Therefore, accuracy assessment and validation of the VIIRS snow cover products are essential and have great significance to the snow scientific community. Moreover, intercomparison of the MODIS and VIIRS snow products is crucial to ensure the smooth transition of snow cover products from MODIS to VIIRS for the successive development of climate data records (CDR) (Riggs et al., 2015; Riggs et al., 2016b).

1.3 Study Purpose and Objectives

The VIIRS instrument on board the Suomi-NPP satellite will provide long-term continuity of several environmental data series including snow cover initiated with the MODIS aboard Aqua and Terra satellites for eventually developing moderate resolution climate data record (CDR). The 375 m spatial resolution of VIIRS offers the potential to provide more accurate map of snow cover extent compared to 500 m MODIS products. The general hypothesis is that the VIIRS and MODIS snow cover products should have similar accuracy for snow cover detection since the same algorithm is used for both instruments (Riggs et al., 2015). However, there are speculations regarding differences between MODIS and VIIRS snow cover products because of different spatial resolution and spectral coverage. However, the quantitative comparisons between VIIRS and MODIS snow products are currently limited. Although there are two sets of VIIRS snow cover products, one developed by NOAA (National Oceanic and Atmospheric Administration) and other by NASA (National Aeronautics and Space Administration), only NOAA VIIRS snow cover product is publicly available for the 2016 hydrological year. Consequently, the overall objective of this study is to compare the MODIS and NOAA VIIRS snow products during the 2016 hydrological year. The general objectives are:

1. To intercompare the daily swath snow cover products from the Aqua MODIS (MYD10L2) and the NOAA VIIRS (VSCMO) to assess their agreement using confusion matrices and qualitative analysis.

2. To identify fractional snow cover (FSC) threshold of the Aqua MODIS swath snow map (MYD10L2) that best approximates the VIIRS binary snow map (VSCMO) using snow omission and commission errors between the two products.

The main purpose of this research is to evaluate the similarities and differences among the snow cover products from the MODIS and VIIRS instruments. To accomplish this research objectives, the swath snow products from two different sources, i.e. MODIS/Aqua Collection 6 (MYD10_L2) and the NOAA VIIRS EDR (VSCMO/binary) were used. The MODIS Aqua swath product is selected over the MODIS Terra snow product because the Aqua satellite carrying MODIS instrument and Suomi NPP satellite carrying VIIRS instrument crosses the equator from south to north (ascending node) each day at the same time i.e. approximately 1:30 P.M. and 1:30 A.M. local time, whereas the Terra satellite cross the equator from north to south (descending node) at approximately 10:30 A.M. and 10:30 P.M. (Ault et al., 2006). Furthermore, the swath product is selected because it is the first order snow product from which other higher level snow products are developed, and their validation is relevant to other higher level snow cover products (Hall and Riggs, 2007). Additionally, only VIIRS swath snow product is currently available. The MODIS snow cover data were obtained online from the Distributed Active Archive Center (DAAC) at the National Snow and Ice Data Center (NSIDC), and the NOAA VIIRS data were obtained from NOAA Comprehensive Large Array-Data Stewardship System (CLASS).

2. LITERATURE REVIEW

2.1 Remote Sensing of Snow Cover

Remote sensing techniques can detect snow cover in the optical, thermal and microwave regions of electromagnetic spectrum (Kunzi et al., 1982; Lucas and Harrison, 1990). Passive microwave remote sensing can provide information on snow cover extent, snow water equivalent (SWE), snow depth, and snow state (wet/dry) since the snowpack is sensitive to microwave radiation (Kunzi et al., 1982). Conversely, active microwave sensors are not ideal for mapping snow since only wet snow can be detected reliably and under the dry snow condition, the surface beneath the snow is more sensitive to active microwave signal compared to snow (Dietz et al., 2012; Wang et al., 2008). Optical remote sensing is the most popular and applicable remote sensing technique for snow cover extent mapping. Snow can be mapped using visible bands (300-700 nm) as snow reflectance is high compared to no-snow reflectance in the visible region of electromagnetic spectrum. Also, the contrast between snow and no-snow surfaces is greater in the visible region compared to near infrared region (Dietz et al., 2012). On the other hand, the discrimination between snow and cloud is difficult in visible spectrum because cloud reflectance is also high in visible portion of electromagnetic spectrum (Hall et al., 2010) and requires information from the short wave infrared (SWIR) region for snow/cloud discrimination (Hall et al., 2002; Ault et al., 2006).

Cloud cover is one of the major limiting factors for detecting snow cover in optical remote sensing since the radiation in visible and infrared spectrum cannot penetrate the clouds (Ault et al., 2006; Key et al., 2013; Xie, et al., 2009). Cloud has a spectral overlap (similar response in visible, infrared and thermal spectrum) with snow that hinders snow/cloud discrimination. Cloud and cloud shadows obscure snow surfaces influencing the spectral albedo of snow (Warren and Wiscombe, 1980). Cloud shadows have low reflectance in SWIR bands similar to snow. Moreover, snow commission error (detecting snow where there is no snow) in optical satellite data is often associated with cloud fringes, and the popcorn-shaped cloud formations over vegetated surfaces (Riggs et al., 2016a). Mixed snow/cloud pixels further increases the snow-cloud confusion. However, Dozier (1989) found that snow can be differentiated from thin clouds in the spectral region from 1.55 to 1.70 μm. Snow reflectance is low in the short wave infrared (SWIR) spectrum while cloud retains a high reflectance, and this criteria helps to discriminate between snow and clouds (Hall et al., 2002; Ault et al., 2006; Riggs et al., 2016a). Crane and Andersen (1984) have recommended using the middle infrared (MIR) spectrum along with visible (VIS) and thermal infrared to differentiate snow and clouds. Furthermore, Bunting and d'Entremont (1982) have highlighted the significance of middle infrared/visible ratio in discriminating snow, clouds and lands. However, this criteria is less effective when cloud coverage is very high. Rodell and Houser (2004) revealed that MODIS scenes with greater than 94% of cloud cover are not suitable for snow detection.

Dense vegetation, particularly conifer forest, that cannot hold snow in its canopy reduces snow reflectance and influences snow detection (Kung et al., 1964). Klein et al. (1998) recommended normalized difference vegetation index (NDVI) to be included in MODIS snow detection algorithm to map snow in forested areas, and suggested to replace MODIS band 6 with MODIS band 7 to compute NDSI. In addition, sensor saturation also inhibits snow observation and snow cover area mapping. The terrain shadows also confuses snow pixels and contaminate snow reflectance. Additionally, other factors such as snow grain shape and size, snow depth, snow impurities, age of snow, temperature, and liquid water content that influences the reflective properties of snow also limits the accurate measurement of snow cover extent (Dietz et al., 2012). The reflectivity of fresh and pure snow, which is up to 90% in visible portion of electromagnetic spectrum, decreases with the increase in snow age (Dietz et al., 2012).

The spatial, temporal and spectral resolution of satellite sensors is also critical in mapping snow cover area (Rango et al., 1983). High spatial resolution allows for more accurate location, discrimination and monitoring of snow cover extent, whereas high temporal resolution increases the likelihood of cloud free images. High temporal resolution also allows for the observation of snow cover variation over short time period. However, there is a tradeoff between spatial and temporal resolution (Dobreva and Klein, 2011). Furthermore, high spectral resolution allows for accurate snow discrimination and measurement of snow properties such as grain size, density, temperature variations snow water equivalent (or depth) and the presence of liquid water in the snowpack (Lucas and Harrison, 1990).

2.2 Binary Snow Cover Mapping

Binary snow cover mapping is a traditional approach where each pixel is mapped as either snow-covered or snow-free (Dobreva and Klein, 2011). In binary snow cover mapping, preferably a pixel is classified as snow when at least fifty percent of its area is snow covered (Hall et al., 2002). Most of the snow detection algorithm is based on the Normalized Difference Snow Index (NDSI). Snow has high reflectance in visible portion of electromagnetic spectrum but low reflectance in SWIR region which enables for the calculation of NDSI (Dozier, 1989; Hall et al., 1995; Dobreva and Klein, 2011) as:

$$\mathrm{NDSI} = (\mathrm{VIS} - \mathrm{SWIR})/(\mathrm{VIR} + \mathrm{SWIR}) \quad (1)$$

NDSI has been used in detecting snow cover from various satellite sensors since 1970s (Riggs et al., 2015). Typically, snow has higher NDSI values than other land covers. In general, a pixel with NDSI greater than 0.0 is considered as snow and a pixel with NDSI equals to or less than 0.0 is considered as no snow (Hall et al., 2002), however all surface features with NDSI greater than 0 are not snow cover (Riggs et al., 2016a). A threshold value of NDSI greater than 0.4 is typically used to highlight snow cover areas (Dozier, 1989) although this value is not universally applicable (Solberg, 2006). Since the NDSI value depends on the differences of VIS and SWIR reflectance, Riggs et al. (2015) demonstrated that the confidence level of snow cover detection increases with increase in their differences. NDSI is very effective in delineating snow cover when the atmosphere is clear, and viewing geometry and solar illumination are decent (Riggs et al., 2016a).

2.3 Fractional Snow Cover Mapping

Fractional snow cover mapping is a sub-pixel based snow cover mapping technique which improves binary snow cover mapping that it can derive more accurate estimates of snow cover area (Dobreva and Klein, 2011). Fractional snow cover mapping can address issues of snow cover mapping from coarse resolution remote sensing data, snow delineation on dense vegetation surfaces and in estimating snow from a pixel with less than 60% snow cover (Hall et al., 1995; Dobreva and Klein, 2011). Snow fraction information has greater significance in the study of snow processes at localized area such as small watersheds, and precise hydrological and climate modelling applications (Salomonson and Appel, 2004).

Researchers have used different approaches and developed new models for fractional snow cover (FSC) mapping. Linear mixture analysis or linear spectral unmixing is most common approach in FSC mapping, which assumes that the reflectance of "a pixel is a linear combination of the surface components within that pixel and that the weight of each component equals the proportion of the pixel's IFOV that contains the component" (Dobreva and Klein, 2011). The performance of linear mixture analysis is determined by availability and quality of endmember (Schowengerdt, 1997). Vikhamar and Solberg (2002) have developed SnowFor model, which is based on a linear spectral mixture analysis. SnowFor is particularly useful for forested areas that discriminate bare, forest and snow-covered surfaces. Painter et al. (2009) developed automated MODIS Snow-Covered Area and Grain size (MODSCAG) model, which can derive fractional snow cover, snow grain size and snow albedo from MODIS reflectance

data. They validated the MODSCAG model using Landsat data where RMSE for snow fraction ranges between 1% and 13% with a mean RMSE of 5%. Similarly, Rosenthal and Dozier (1996) developed a decision-tree (regression tree test) based classification model to map fractional snow cover from Landsat TM data with similar accuracy to aerial photograph based snow maps. The Norwegian Computing Center developed NLR (Norwegian Linear-Reflectance to-snow-cover) algorithm to derive snow fractions in the mountain region above tree line from AVHRR data (Solberg and Andersen, 1994; Dietz et al. 2012). The Finnish Environment Institute (SYKE) developed SCAmod algorithm to calculate snow fractions for open areas and forested regions, which was first applied to AVHRR data (Dietz et al. 2012).

Another approach in FSC mapping is an empirical approach by developing empirical relationship between satellites observed reflectance and measured snow fraction where endmembers are not required (Solberg et al., 2006). Salomonson and Appel (2004; 2006) used an empirical Normalized Difference Snow Index (NDSI) technique to derive fractional snow cover information from MODIS data. They derived the snow fraction in each MODIS pixels using an ordinary least-squares regression approach. Enhanced Landsat Thematic Mapper-Plus (ETM+) was used as a ground truth data to develop linear relation between NDSI and fractional snow cover within a MODIS pixel. This approach was tested over Alaska, Siberia and Labrador and the results indicated reasonable robust relationship between fractional snow cover and NDSI with mean absolute error less than 0.1 over the range of 0.0 to 1.0 fractional snow cover. This approach was used to produce MODIS Collection 5 fractional snow cover products

(FSC). However, this approach can be limited in estimating snow fraction in heavily forested areas (Dobreva and Klein, 2011).

The Artificial Neural Network (ANN) is a machine learning approach that can handle both linear and nonlinear mixing components, does not require spectral endmember information, and can incorporate auxiliary information such as land cover type. Dobreva and Klein (2011) used ANN to estimate snow cover fraction from MODIS data at different land cover classes, however, did not find major improvement in snow fraction mapping over forest areas when compared with the MODIS snow fraction products.

2.4 MODIS Snow Cover Products

MODIS snow cover products are available at different spatial and temporal scales. The 5-minute swath product (MOD10L2 and MYD10L2) with 500 m spatial resolution and nominal swath coverage of 2330 km (across track) by 2030 km (along track) is the first order snow product from which other higher level snow products are developed (Hall and Riggs, 2007; Riggs et al., 2016a). The higher level snow products include the daily snow cover product (MOD10A1 and MYD10A1) and eight day snow product (MOD10A2 and MYD10A2) at 500 m spatial resolution in a sinusoidal projection, and the daily global climate modeling grid (CMG) snow product (MOD10C1 and MYD10C1), the eight-day climate-modeling grid (CMG) snow-cover data product (MOD10C2 and MYD10C2), and monthly snow cover product (MOD10CM and MYD10CM) at 0.05 degree spatial resolution (Riggs et al., 2016a). A detailed

explanation of all the snow products is available in the MODIS Snow Products Collection 6 (C6) User Guide (Riggs et al., 2016a).

The MODIS snow detection algorithm is based on the ratio of the difference in VIS and SWIR reflectance, termed as the Normalized Difference Snow Index (NDSI) by Hall et al. (1995), which is very effective for detection and mapping of snow, cover area from the Earth surface (Hall et al., 2001). The visible band (band 4) and shortwave infrared band (band 6) of the MODIS are useful for developing the global snow cover maps (Hall et al., 2002), where VIS band ranges from 0.545 μm to 0.565 μm and SWIR band ranges from 1.628 μm to 1.652 μm, both at 500 m spatial resolution (Ault et al., 2006). A threshold value of NDSI greater than 0.4 was typically used to indicate binary snow cover in earlier version of MODIS snow cover products (Riggs et al., 2016b).

Collection 6 represents the recent version of MODIS snow cover products. The major change in the C6 snow products is that fractional snow cover (FSC) datasets of previous versions has been replaced by the NDSI snow cover that uses the entire NDSI range from 0.0 to 1.0 (Riggs et al., 2016a). The NDSI snow cover dataset represents the presence of snow in a pixel that ranges from 0-100%. Moreover, the snow cover binary map that was generated using 0.4 threshold recommended by Dozier (1989) has been removed in the recent version of MODIS snow products since this value was not applicable in all areas (Riggs et al., 2016b).

The MODIS snow cover algorithms and data products have been revised and improved since the launch of the instrument although NDSI has always been used as the basis for snow cover detection and mapping (Riggs et al., 2016a). Several data screens

such as low VIS reflectance screen, low NDSI screen, high SWIR reflectance screen and solar zenith screen are applied in the algorithm to alleviate the snow commission and omission errors (Riggs et al., 2016a). Additionally, the Unobstructed Field of View (UFOV) cloud mask flag from the MODIS cloud mask product is used to mask clouds (Riggs et al., 2016a). A detailed explanation of algorithm is available in the NASA MODIS Algorithm Theoretical Basis Document (ATBD) for the MODIS Snow and Sea Ice-Mapping Algorithms (Hall et al., 2001; Riggs et al., 2015).

2.5 VIIRS Snow Cover Products

The main objective of developing VIIRS snow cover products is to ensure the long-term continuity of satellite snow cover maps for the subsequent development of a climate-data record (CDR) (Justice et al., 2013; Riggs et al., 2016b). The heritage MODIS snow cover algorithm is the foundation for the VIIRS snow cover algorithm and products (Riggs et al., 2015). So, NDSI is the basis for VIIRS snow detection algorithm and computed using VIIRS band I1 (0.64 μm), and band I3 (1.61 μm), both at 375 m spatial resolution.

There are two sets of VIIRS snow cover products, one developed by NOAA (National Oceanic and Atmospheric Administration) and other by NASA (National Aeronautics and Space Administration).

The NASA's VIIRS snow cover algorithm and products are similar to the MODIS Collection 6 (C6) algorithms and data products, although there are some differences due to sensor spatial resolution and band location and width (Riggs et al.,

2015; Riggs et al., 2016b). The detail explanation of NASA VIIRS snow algorithm is available in the VIIRS Snow Cover Algorithm Theoretical Basis Document (Riggs et al., 2015). The NASA VIIRS snow products also does not include Snow Cover Area (SCA) and Fractional Snow Cover (FSC) data arrays. The VIIRS snow cover products are available at different spatial and temporal scale. The Level 2, 6-minute swath product (VNP10L2) has a spatial resolution of 375 m with nominal swath coverage of 6400 pixels (across track) by 6464 pixels (along track) (Riggs et al., 2016b). The other snow products include Level 2G daily tiled snow product (VNP10L2G), Level 3 daily (VNP10A1) and 8-day snow cover product (VNP10A2) of 375 m resolution with a sinusoidal projection, and Level 3 daily global climate modeling grid (CMG) snow product (VNP10C1) at 0.05 degree spatial resolution. The detail explanation of all the snow products is available in the NASA S-NPP VIIRS Snow Products Collection 1 User Guide (Riggs et al., 2015; Riggs et al., 2016b). The NASA VIIRS swath snow product (VNP10L2) is publicly available since July 2017.

NOAA's VIIRS (VIIRS/NOAA) snow cover products are developed based on MODIS Collection 5 (C5) snow cover algorithms, and are thus different than NASA's VIIRS snow products (Riggs et al., 2016b). The VIIRS/NOAA snow cover products include the VIIRS Snow Cover Binary (snow/no snow) EDR and the VIIRS Snow Cover Fraction EDR (Justice et al., 2013; Key et al., 2013). The VIIRS Snow Cover Binary has a spatial resolution of 375 m. It is generated using the heritage MODIS Snow Map algorithm (Hall et al., 2001), which categorizes a pixel as snow or no snow based on NDSI values, and snow detection is limited to an NDSI range of 0.4 to 1.0 (Baker, 2011;

Justice et al., 2013). The VIIRS Snow Cover Fraction EDR is produced by spatially aggregating Binary Snow Cover EDR within 2 x 2 adjacent pixel cells to generate five classes of fractional snow cover at and 750 m spatial resolution: 0, 25, 50, 75 and 100 % (Baker, 2011; Justice et al., 2013; Key et al., 2013). The accuracy requirement for Snow Cover Binary EDR is 90% probability of correct typing (Justice et al., 2013; Key et al., 2013). Similar to the MODIS, snow identification is limited to clear sky conditions as clouds are opaque in visible and infrared bands (Key et al., 2013). Among the four categories of cloud confidence flag such as confidently cloudy, probably cloudy, probably clear and confidently clear, VIIRS snow cover maps were generated using 'confidently clear' cloud mask (Justice et al., 2013; Key et al., 2013). The VIIRS Snow Cover Fraction EDR is less accurate than the Binary EDR and has limited utility (Justice et al., 2013). The detail explanation of NOAA's VIIRS snow cover products is available in JPSS VIIRS snow cover ATBD (Baker, 2011; Romanov, 2015).

2.6 Validation of MODIS and VIIRS Snow Products

Various studies have been conducted to evaluate the accuracies and limitations of the MODIS snow cover extent products over several regions of the world during different time periods. A few of the key studies are described here. Klein and Barnett (2003) validated the MODIS daily snow cover products for the 2000-2001 snow season over the Upper Rio Grande River Basin by comparing with the National Operational Hydrologic Remote Sensing Center (NOHRSC) snow cover maps and in-situ Snowpack Telemetry (SNOTEL) measurements. They demonstrated good overall agreement

between the MODIS and NOHRSC snow maps, and between the MODIS and *in-situ* SNOTEL measurements with an overall accuracy of 86% and 94% respectively during cloud free days. Additionally, their studies revealed that MODIS algorithm mapped a slightly higher portion of the basin as snow covered compared to NOHRSC approach, and the Kappa coefficient statistics was 0.721 representing a substantial level of agreement between MODIS and SNOTEL, which indicates that both approaches are similar in their ability to map snow. However, the Kappa coefficient for MODIS snow maps when compared against *in-situ* SNOTEL measurements was 0.589 indicating moderate level of agreement according to the Landis and Koch (1977) guidelines.

Parajka and Bloschl (2006) validated the MODIS daily snow products (version 4) against the daily in situ measurements of snow depth over Austria for the period between February 2000 and December 2005, and indicated very good agreement with an overall accuracy of about 95% on cloud free days. Furthermore, they evaluated the spatial and temporal variability of MODIS data over Austria. They demonstrated that the spatial extent of the snow cover was only 7% while cloud cover was 63% on average, citing cloud as limiting factor for the MODIS snow products. Moreover, their evaluation on the seasonal variation of the MODIS snow mapping against the climate station data indicated that the lowest agreement occurs during winter months (around 55%) due to cloud cover.

Ault et al. (2006) evaluated the MODIS daily swath product (MOD_L2) and cloud mask (MOD35) using field observations of snow depth, snow water equivalency, cloud type, and total cloud cover from the SATELLITES (Students And Teachers

Evaluating Local Landscapes to Interpret The Earth from Space) and GLOBE (Global Learning and Observations to Benefit the Environment) programs and daily snow depth measurements from the National Weather Service (NWS) Cooperative Observing Stations. The study was conducted over the Lower Great Lake Region during 2001-2003, which demonstrates that an overall deterministic accuracy of daily swath snow product was 92.3% and Kappa coefficient (K_{hat}) value was 79.2% when compared with the field observation, and an overall accuracy of 85.6% and K_{hat} value of 70.9% when compared with NWS observations during clear sky condition. The highest error occurred in the forested areas and the areas with trace amount of snow depth under 10 mm (only 41% accuracy).

In order to address the issue of clouds in the MODIS snow products, Wang et al. (2009) developed an algorithm to combine the MODIS Terra and Aqua snow cover products to generate cloud-less or cloud-low daily and 8-day snow products, and evaluated against snow depth measurements. The logic was that since the Aqua and the Terra satellites crosses the equator at different time period, the cloud blockade would not be there at the same time. The study was conducted over northern Xinjiang, China from 1 September 2003 to 31 August 2004. Their studies discovered that the combined snow products had greater accuracy compared to the original snow products. Furthermore, they also inter-compared the MODIS Terra and Aqua snow cover products, and revealed that the accuracy of Terra snow products was slightly better than the Aqua snow products. Similarly, the agreement of snow classification was higher (close to 100%) in the winter months (November-March) and lower in the summer and spring months

(April-October), and the major disagreement was found in the transition zone (snow-land) for both products.

Xie et al. (2009) also used similar approach over Colorado Plateau, USA and Northern Xinjiang, China for 2003-2004 hydrological year. They combined the daily MODIS Terra and Aqua snow cover products to generate new snow cover imageries, and validated the snow products against daily snow water equivalent (SWE) data. They found that overall the MODIS composite snow products had much higher agreement with ground measurements compared to individual Terra and Aqua snow products. Thus, the combination of Terra and Aqua snow products has more potential to generate cloud free snow cover images.

Compared to the extensive validation of MODIS snow cover products, the evaluation and validation of VIIRS snow products are currently at early phase. Key et al. (2013) evaluated the NOAA VIIRS snow cover binary maps generated during December 2012 – May 2013 based on comparison with corresponding false color imagery for qualitative assessment, and with *in situ* snow observations at ground-based stations for quantitative assessment. The binary snow maps were also compared with snow and ice cover charts generated with NOAA Interactive Multisensor Snow and Ice Mapping System (IMS), and MODIS snow maps. The visual comparison with false color imagery revealed good agreement with the major patterns of the global snow cover distribution and the inconsistencies were found in the forested area (boreal forest zones in Canada and Far East Russia), particularly during late spring due to low illumination of old melting snow. The quantitative comparison of VIIRS binary snow cover maps with the

ground station data over conterminous United States (CONUS) area showed good agreement between them with 93 to 98% agreement during winter season, and less the agreement (about 90%) during beginning and end of the winter and in spring season.

The binary snow map meets the accuracy requirements with respect to the Joint Polar Satellite System (JPSS) Level 1 Requirements Documents. The quantitative comparison of VIIRS snow maps with IMS daily snow maps over the confidently clear regions demonstrated about 99% agreement during most of the winter 2012-2013 and about 95% during late spring (May). However, Key et al. (2013) underlined that VIIRS and IMS comparison cannot be considered true validation since the IMS snow map products does not represent direct snow cover measurements. The VIIRS binary snow map showed similar and sometimes higher accuracy than the MODIS snow data, however it was also revealed that more clouds are mapped in the VIIRS snow product (65-70%) than MODIS products (55-60%) as depicted by Wang et al. (2009) resulting smaller areal coverage of VIIRS daily snow maps. Furthermore, even during the clear atmosphere, the transition zone between snow and land is often recorded as cloudy in the VIIRS snow map, and they concluded that conservative VIIRS cloud mask was one of the reasons for its better accuracy. So, the nature of cloud mask needs to be integrated during the validation of satellite snow cover products (Key et al., 2013).

In NASA VIIRS user guide, Riggs et al. (2015) states that the accuracy of NASA VIIRS snow products was 95% under ideal condition based on the visual analysis with imagery and comparison with snow cover maps from other satellites. They also hypothesized that the accuracy of NASA VIIRS snow cover product is very similar to

the heritage MODIS C5 and C6 snow cover products. Moreover, there are theories regarding the similarity and difference between MODIS and VIIRS snow cover products because of their different spatial resolution and spectral coverage. However, the quantitative comparisons between VIIRS and MODIS snow products are currently limited. So, validation and intercomparison of VIIRS-MODIS snow cover products are very essential to ensure the long-term continuity of MODIS snow products.

3. METHODOLOGY

3.1 Study Area

The study area includes portion of Central and Western Canada and Midwestern United States, which lies roughly between 38.29º - 52.71ºN and 80.92º - 104.75ºW (Fig. 1) and covers approximately 2,528,690 square km. The study area covering Canadian provinces include portions of Ontario, Manitoba and Saskatchewan while the Midwestern United States includes Iowa, Minnesota, Wisconsin and parts of Illinois, Indiana, Kansas, Michigan, Missouri, Nebraska, North Dakota, Ohio, and South Dakota. The study area is representative of seventeen International Geosphere-Biosphere Programme (IGBP) land cover types including evergreen needleleaf and broadleaf forest, deciduous needleleaf and broadleaf forest, mixed forest, open and closed shrublands, grasslands, woody savannas, cropland and natural vegetation mosaic, croplands, urban and built-up, permanent wetlands, water, snow and ice, and barren or sparsely vegetated (Fig. 1). Croplands is the most dominant land cover types covering 35% of total area followed by mixed forest (15%), cropland/natural vegetation (14%) and grasslands (13%). Water and wetlands comprises of about 10% of total area. The land cover map for the study area was obtained from the Global Land Cover Facility (GLCF), which is 2013 MODIS land cover type data product (MCD12Q1) in the IGBP Land Cover Type Classification with 500 m spatial resolution (Friedl et al., 2010; Channan et al., 2014).

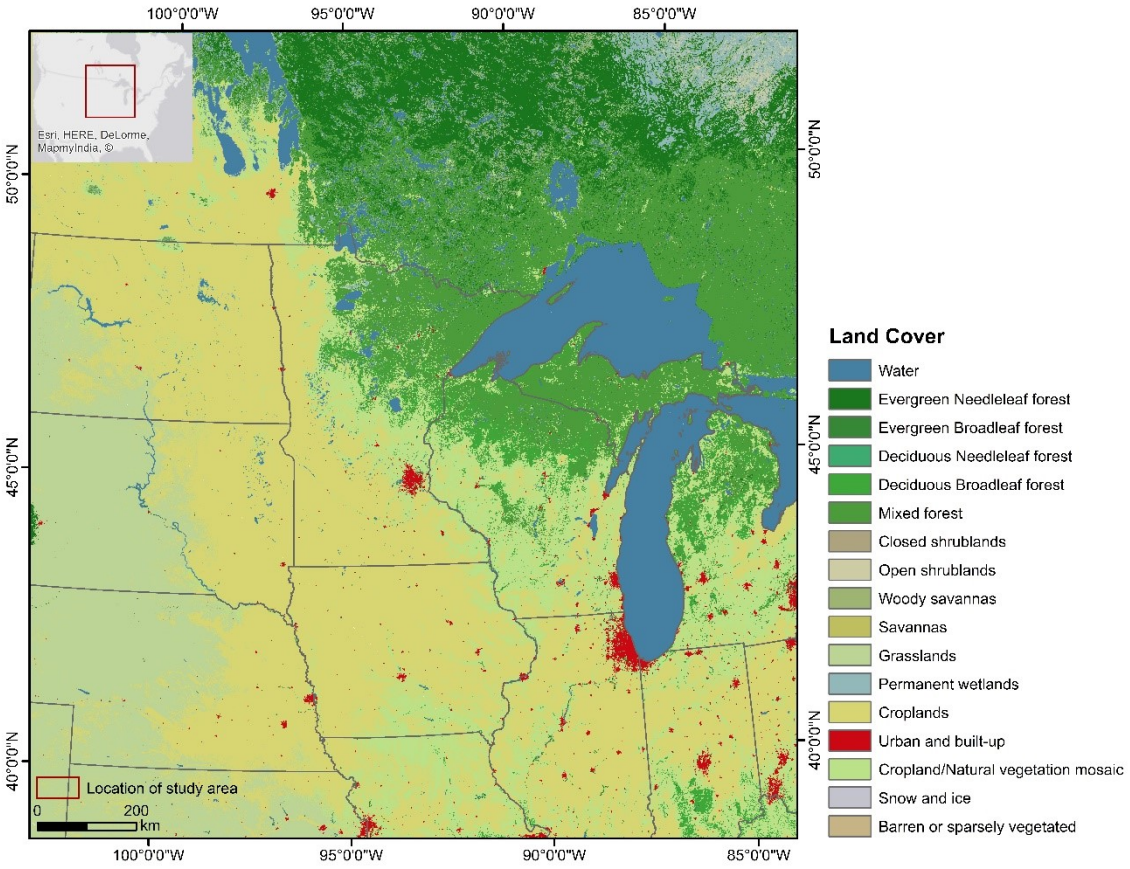

Fig. 1. Study Area with Land Cover Types.

3.2 Data Description

The swath snow products come from two different sources, i.e. MODIS/Aqua Collection 6 (MYD10L2) and NOAA VIIRS EDR (VSCMO/binary) and encompasses the 2016 hydrological year (snow season) from 1 October 2015 to 31 May 2016, which includes 244 snow cover maps from MODIS and VIIRS.

3.2.1 MODIS Snow Product – MYD10L2

The MODIS/Aqua swath snow product (MYD10L2) is a Level 2 snow product. The MODIS snow algorithm uses different MODIS Aqua data products such as MYD02HKM (MODIS/Aqua Calibrated Radiances 5-min L1B Swath 500 m) and MYD021KM (MODIS/Aqua Calibrated Radiances 5-min L1B Swath 1 km) band radiance data (31 bands), MYD03 (MODIS/Aqua Geolocation Fields 5-min L1A Swath 1 km) geolocation data, and MYD35L2 (MODIS/Aqua Cloud Mask and Spectral Test Results 5-min L2 Swath 250m and 1km) to produce the MYD10L2 snow products (Riggs et al., 2016a). The data utilized from MYD02HKM utilized radiance bands 1 (0.645 μm), 2 (0.865 μm), 4 (0.555 μm) and QIR 6 (1.640 μm), and the data from MYD021KM utilized radiance band 31 (11.03 μm). The data from MYD03 includes land/water mask, solar zenith angle, latitude, longitude and geoid height, and the data from MYD35L2 includes unobstructed field of view flag and day/night flag (Riggs et al., 2016a). The Scientific Data Sets (SDS) of MYD10L2 C6 includes NDSI Snow Cover, NDSI Snow Cover basic quality assessment (QA), NDSI Snow Cover Algorithm Flags QA, NDSI, and Latitude and Longitude data in a compressed HDF_EOS format (HDF4) (Riggs et al., 2016a). Only the NDSI Snow Cover dataset is used for this study. The NDSI Snow Cover has the coded integer values which represent different features. For example, NDSI Snow has values ranging from 0-100% that characterize the percentage of snow cover in a pixel (Riggs et al., 2016a). All the features of the NDSI Snow Cover dataset with their unique values are listed in Table 1.

Table 1. Features of the NDSI Snow Cover SDS (Riggs et al., 2016a)

Features	**Key value**
NDSI snow fraction	0-100%
Missing data	200
No decision	201
Night	211
Inland water	237
Ocean	239
Cloud	250
Detector saturated	254
Fill	255

3.2.2 VIIRS Snow Products – VSCMO

The VSCMO is an Environmental Data Record (EDR) Level 2 product. The inputs for VSCMO includes VIIRS TOA reflectance bands for I1 (0.640 μm), I2 (0.865 μm), and I3 (1.61 μm) at 375 m spatial resolution, brightness temperature band I5 (11.450 μm) at 375 m, geolocation files (solar and sensor zenith angle), aerosol optical thickness (AOT) intermediate product (IP) at 750 m, cloud mask IP, and cloud optical thickness (COP) IP at 750 m spatial resolution (Reed, 2013). The VSCMO is integrated with GITCO file (VIIRS Image Bands SDR Ellipsoid Terrain Corrected Geolocation) in a compressed HDF4 format. The GITCO-VSCMO includes Snow Cover Binary Map

along with geolocation files such as Height, Satellite Azimuth Angle, Satellite Range, Satellite Zenith Angle, Solar Azimuth Angle, and Solar Zenith Angle. However, only the Snow Cover Binary Map is used for this study, and the value of Snow Cover Binary Map includes 0 representing snow free pixels, 1 representing snow pixels, and 255 representing fill value (Reed, 2013).

3.3 Data Preprocessing

Data processing includes the major steps. First, the Modis Conversion Toolkit (MCTK) in ENVI IDL8.3 was used to automatically extract the NDSI Snow Cover dataset from MYD10L2 and reproject the dataset into a North America Albers Equal Area Conic projection using nearest neighbor resampling. MCTK is an HDF file conversion and projection plugin that can be run in ENVI and IDL, which facilitates extraction and projection of the target data (White, 2016a). The Albers Equal Area Conic projection preserves areal measurements and is often used in snow mapping analysis (Huang et al., 2011). Second, the NDSI Snow Cover dataset of MYD10L2 were oversampled to a spatial resolution of 375 m using nearest neighbor resampling to match the spatial resolution of VIIRS snow maps in ENVI IDL8.3. Third, the VIIRS Conversion Toolkit (VCTK) in ENVI IDL8.3 was used to extract the Snow Cover Binary Map from GITCO-VSCMO, and reproject the dataset into the North America Albers Equal Area Conic projection using nearest neighbor resampling similar to MODIS in step 1. The VCTK is a plugin similar to MCTK that can be used to convert, extract and project VIIRS HDF files (White, 2016b). Fourth, the extracted datasets were

mosaicked based on matching dates, clipped to study area extent and saved in Geotiff file format using ArcGIS 10.5 software. Fifth, MODIS water mask, which was resampled to 375 m from 250 m resolution using nearest neighbor resampling, was applied to the datasets to extract only land pixels using ArcGIS 10.5. The water pixels were not included in analysis because the MYD10L2 mapped some water pixels as snow. Fig. 2 illustrates the flowchart of the methodology.

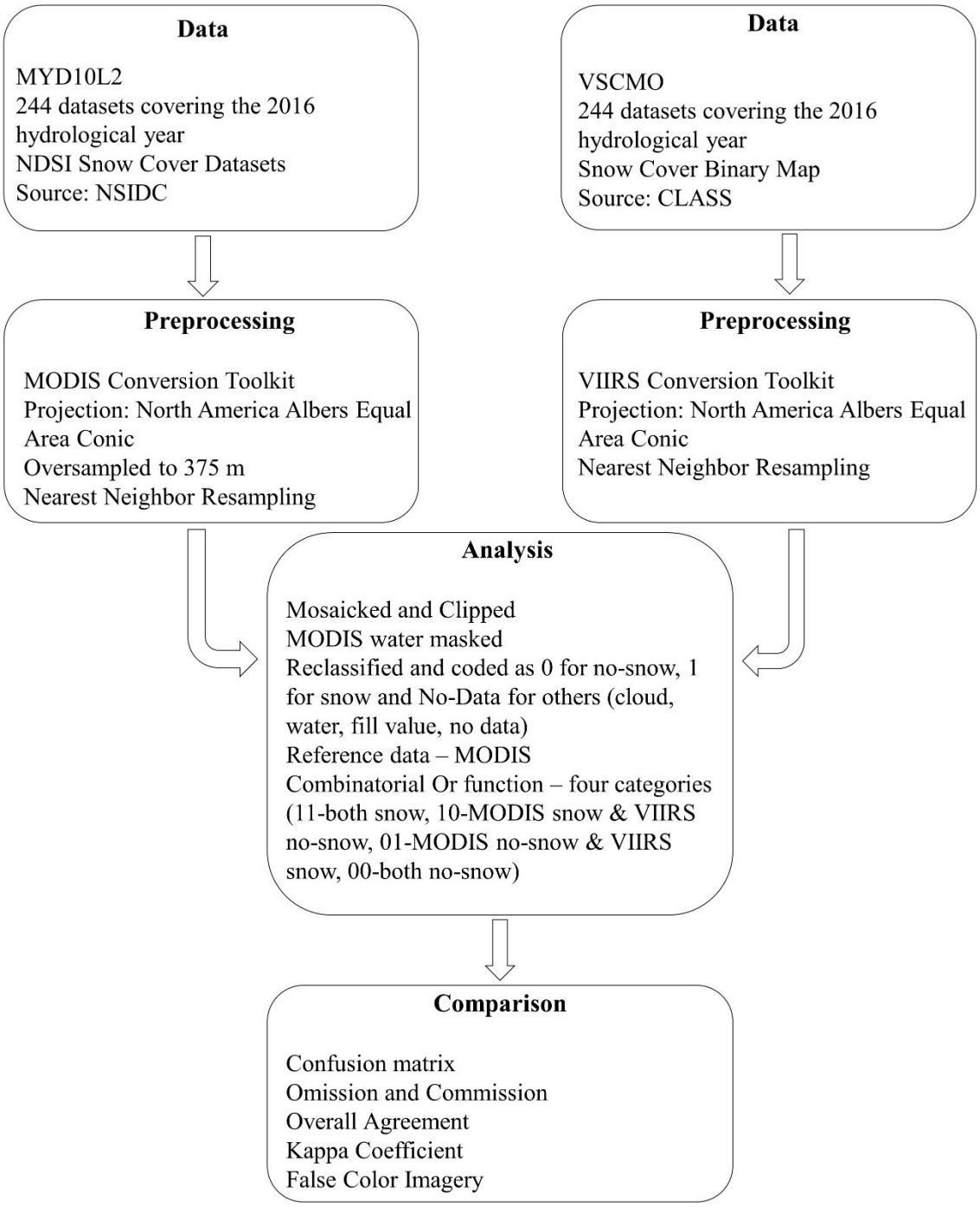

Fig. 2. Flow chart of methodology. The figure illustrates the steps to intercompare MODIS and VIIRS snow products.

3.4 Data Analysis

The NDSI Snow Cover dataset of MYD10L2 includes the information on snow cover fraction as NDSI Snow layer with its value ranging from 0-100% (Riggs et al., 2016a). This layer was converted into Snow Cover Binary Maps by thresholding to facilitate comparison with the VIIRS Snow Cover Binary Map. Different fractional snow cover thresholds (20%, 30%, 40% and 50%) were examined for the binary conversion of MODIS NDSI Snow Cover dataset (Fig. 3). For example, in 20% thresholding, NDSI Snow Cover value of 20% or less is considered as no-snow pixels, and NDSI Snow Cover value greater than 20% is considered as snow pixels. All the other values of the NDSI Snow Cover dataset such as missing data, no decision, night, water, cloud, detector saturation and fill value were categorized as no-data (Fig. 3). The VIIRS Snow Cover Binary Map is in the binary form, and thresholding is not required.

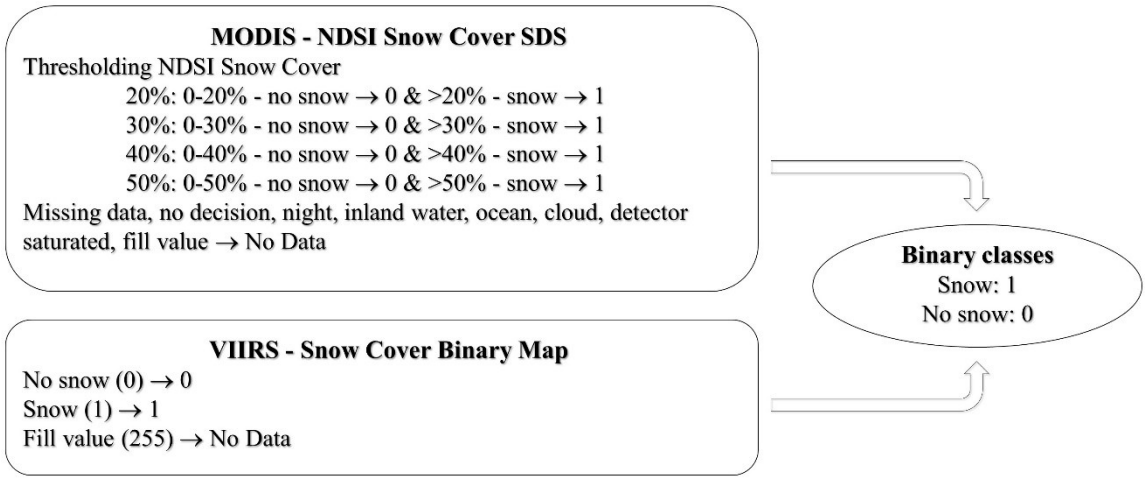

Fig. 3. MODIS and VIIRS snow map reclassification.

MODIS and VIIRS snow binary maps were then recoded/reclassified into binary categories of snow and no-snow. The snow pixels were coded as value 1 and no-snow pixels were coded as 0. Then, the reclassified MODIS and VIIRS snow maps were combined using map algebra operation (Combinatorial OR function in ArcGIS 10.5) to create a series of daily snow maps in which pixels were classified into four different categories based on the decision rules highlighted in Table 2: (1) MODIS snow and VIIRS snow, (2) MODIS snow and VIIRS no-snow, (3) MODIS no-snow and VIIRS snow, and 4) MODIS no-snow and VIIRS no-snow. This approach is adapted from Klein and Barnett (2003), Parajka and Bloschl (2006) and Wang et al. (2009). The comparison was done for 244-days during the 2016 hydrological year (Oct. 1, 2015-May 31, 2016).

Table 2. Decision rules based pixel classification with coded values

MODIS pixels	VIIRS pixels	Output category
1	1	Both snow (11)
1	0	Modis snow-VIIRS no-snow (10)
0	1	Modis no-snow-VIIRS snow (01)
0	0	Both no-snow (00)

Using the computed MODIS Binary snow map as the reference, the snow and no-snow omission and commission were calculated and their average values were plotted with respect to the fractional snow cover thresholds to find optimal MODIS FSC threshold for the MODIS-VIIRS snow map intercomparison.

3.5 MODIS-VIIRS Comparison

A confusion matrix, which is an effective way of representing the accuracy of remote sensing data classification (Congalton, 1991), was used for quantitative comparison between MODIS and VIIRS snow maps. MODIS was used as the reference/ground truth data since it is an established dataset compared to VIIRS. The confusion matrix was also used to determine the Kappa coefficient (K_{hat}), level of agreement (both mapping snow) and disagreement (only one approach mapping snow i.e. commission/inclusion and omission/exclusion errors) and the overall agreement between MODIS and VIIRS snow maps. The Kappa coefficient (K_{hat}) test statistics (Cohen, 1960) delivers improved accuracy measurement of remote sensing image classification as it accounts for both agreement and disagreement information of classification (Klein and Barnett, 2003). Omission or exclusion errors refers to those pixels that belongs to the class of interest but the classifier has failed to identify, while commission errors refers to those pixels from other classes that classifier has labelled as belonging to the class of interest (Richards, 1999).

For qualitative analysis, MODIS and VIIRS snow cover maps were compared with their corresponding false color imagery. Furthermore, to assess the differences in snow mapping between MODIS and VIIRS, comparison maps for selected individual days of interval during the 2016 hydrological year was produced (Klein and Barnet, 2003).

4. RESULTS

Two hundred forty four daily swath snow maps from MODIS and VIIRS were intercompared for 2016 hydrological year running from October 1, 2015 to May 31, 2016 using confusion matrices and qualitative analysis. An appropriate NDSI threshold was selected to create a MODIS binary snow map to compare to VIIRS through minimization of commission and omission errors between the two sets of snow maps. In the results, MODIS served as the reference as this product is both well established and well validated while VIIRS snow products are recently available and its validation is at early phase. The validation was based on snow commission and omission errors, overall agreement and k_{hat} as well as through qualitative analysis of the resulting maps illustrating agreements and commission/omission in conjunction with false color composites of the companion MODIS and VIIRS optical images.

4.1 MODIS Fractional Snow Cover Threshold

The optimal fractional snow cover threshold of the MODIS swath snow map was determined by examining snow cover area at four different FSC thresholds (20%, 30%, 40% and 50%) and comparing the resulting binary snow maps with those of VIIRS. There was tradeoff between the snow and no-snow cover area with the change in snow cover fraction thresholds. The snow cover area in MODIS increases with any decrease in the selected threshold value and vice-versa (Figs. 4 & 5).

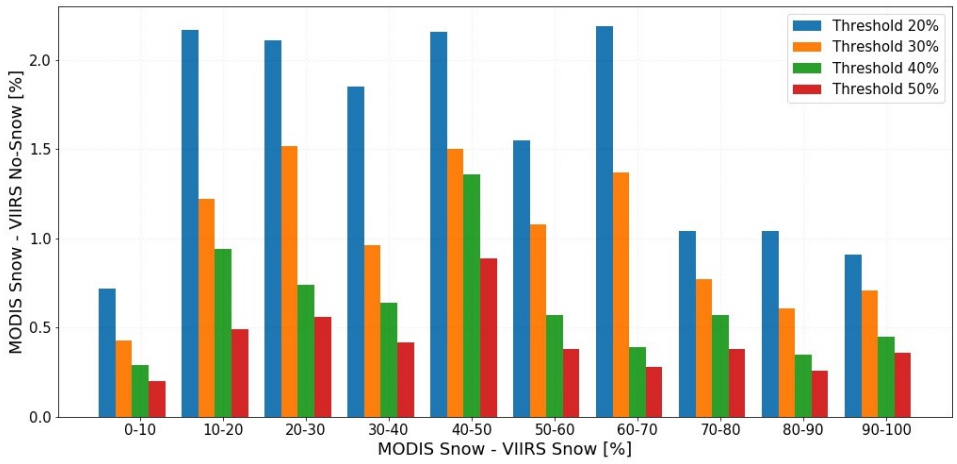

Fig. 4. Bar plots illustrating MODIS snow – VIIRS no-snow (MODIS commission) with respect to MODIS snow – VIIRS snow (agreement) for different snow cover fraction thresholds.

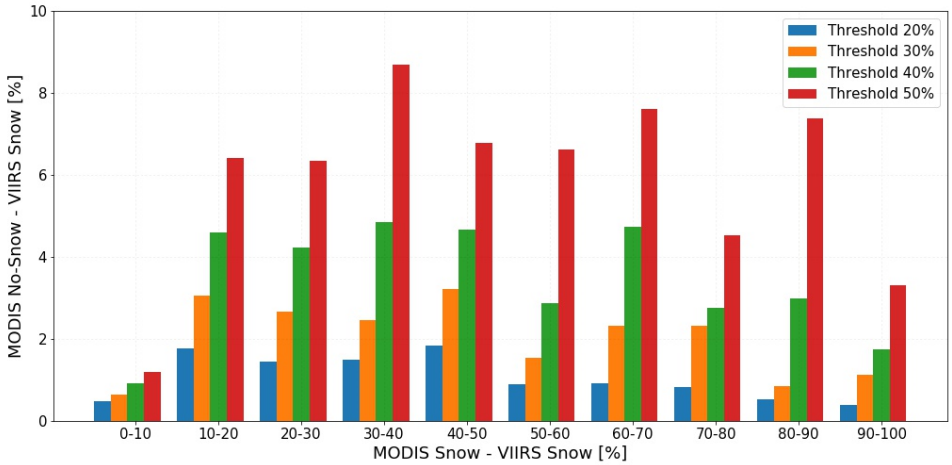

Fig. 5. Bar plots showing MODIS no-snow – VIIRS snow (MODIS omission) with respect to MODIS snow – VIIRS snow (agreement) for different snow cover fraction thresholds.

Similarly, a trade-off between snow commission and omission was observed with changes in FSC thresholds. The average snow commission and omission was plotted against the four FSC threshold values to determine the optimal MODIS NDSI Snow Cover threshold. From Fig. 6, it is evident that the MODIS snow commission and snow omission was equal when the NDSI Snow Cover threshold was near 30%. Therefore, a 30% MODIS NDSI Snow Cover threshold was chosen to produce MODIS binary snow map for comparison with VIIRS. The MODIS NDSI Snow Cover dataset represents snow cover fractions in the range of 0-100% (Riggs et al., 2016a).

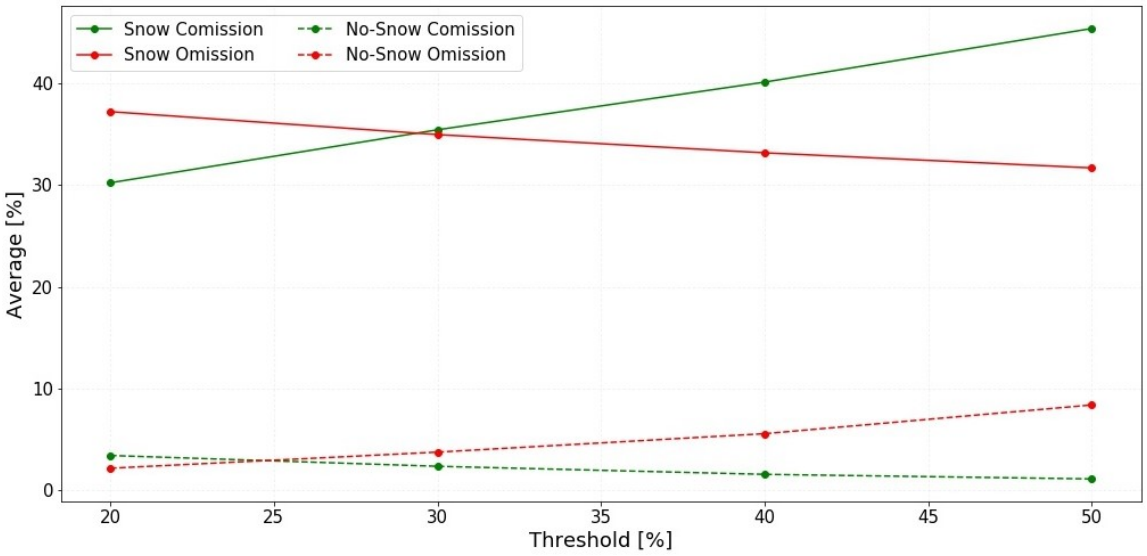

Fig. 6. Line plots showing average snow and no-snow commission and omission between MODIS (reference) and VIIRS snow maps with respect to different snow cover fraction thresholds.

4.2 Total Snow, No-Snow and Cloud

Total snow, no-snow and cloud pixels were determined individually for all 244 MODIS and VIIRS binary snow maps. Fig. 7 represents total snow, no-snow and cloud pixels over the study area during the study period for MODIS and VIIRS snow map. When comparing all the pixels in each day of the 2016 hydrological year, total no-snow area was similar in the MODIS and VIIRS snow maps, whereas MODIS was mapping more clouds and less snow compared to VIIRS, significantly during winter and spring season (Fig. 7).

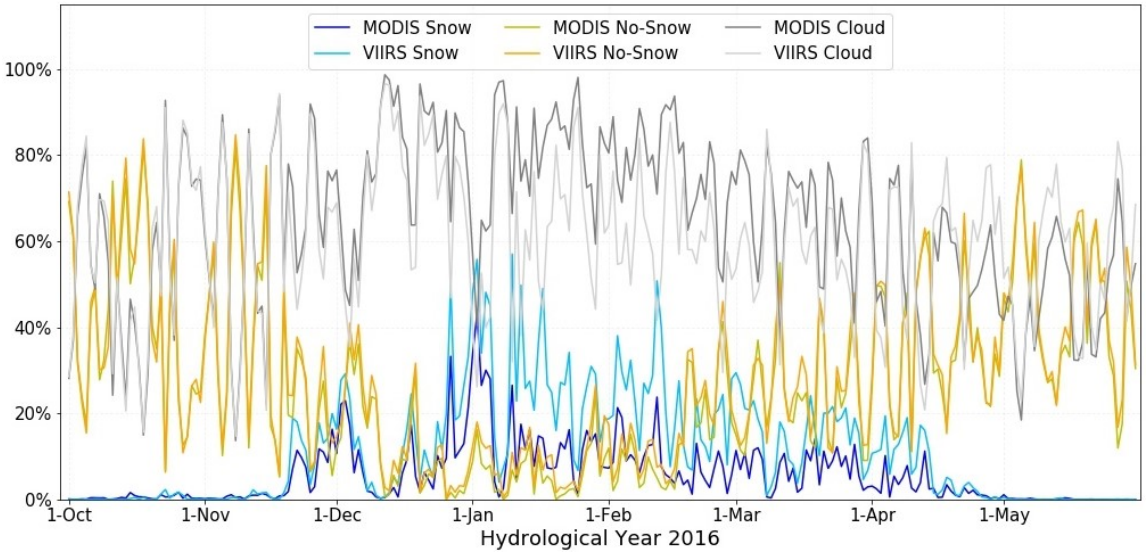

Fig. 7. Line plots illustrating MODIS and VIIRS total snow, no-snow and cloud pixels with respect to each day of the 2016 hydrological year.

Table 3 demonstrates the average percentages of snow, no-snow and cloud portions on MODIS and VIIRS daily swath snow products during the 2016 hydrological

year. The average area of snow in MYD10L2 and VSCMO were 5.72% and 11.43%, no-snow 26.65% and 28.67%, and cloud 65.02% and 59.91%, respectively. It is evident that, on average, VIIRS has more snow and no-snow pixels but less cloud pixels compared to MODIS.

Table 3. Percentage of total snow, no-snow and cloud fractions of the MODIS and VIIRS daily swath snow products in the study area during the 2016 hydrological year

	MODIS (MYD10L2)			VIIRS (VSCMO)		
	Snow	No-Snow	Cloud	Snow	No-Snow	Cloud
Min	0.01	0.01	13.69	0.00	0.19	14.70
Max	43.14	81.96	98.69	57.04	84.74	96.58
Mean	5.72	26.65	65.02	11.43	28.67	59.91
STD	7.08	20.12	19.36	12.81	19.98	17.96

Cloud is one of the limiting factor for optical snow cover area mapping in this study. The scatter plot between VIIRS and MODIS cloud pixels (Fig. 8) indicated more MODIS cloud pixels than VIIRS. On average, MODIS has about 65% of cloud cover while VIIRS has about 60% of cloud cover during the study period.

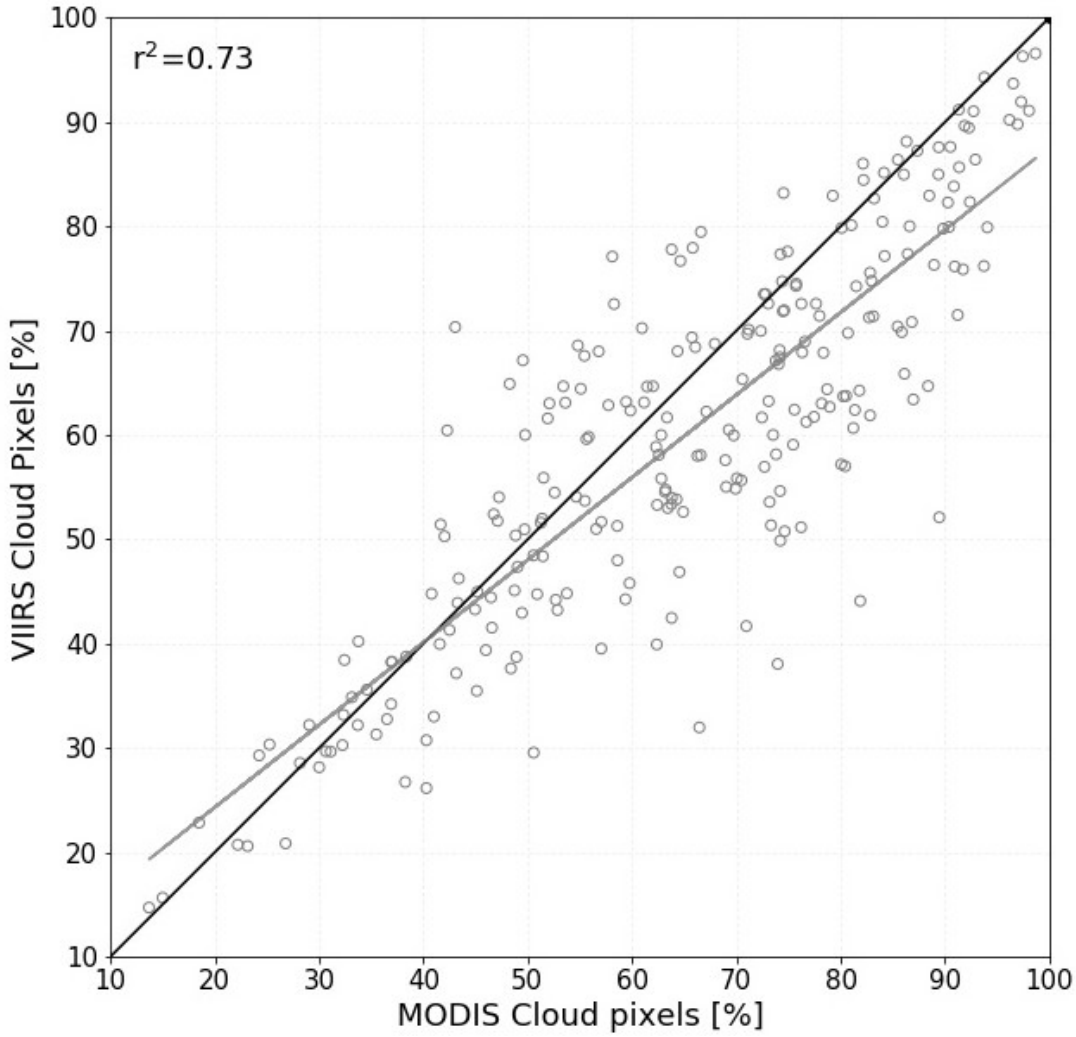

Fig. 8. Scatter plots illustrating VIIRS cloud pixels with respect to MODIS cloud pixels. The gray line represents a first degree polynomial fit while black line indicates a 1:1 relationship.

Furthermore, Fig. 9 depicts that VIIRS consistently maps more snow, and also has less no-snow pixels than MODIS when cloud pixels were excluded from analysis. On average, snow pixels of MODIS and VIIRS comprises of 24.45% and 31.15%, and no-snow pixels comprises of 75.55% and 68.85%, respectively.

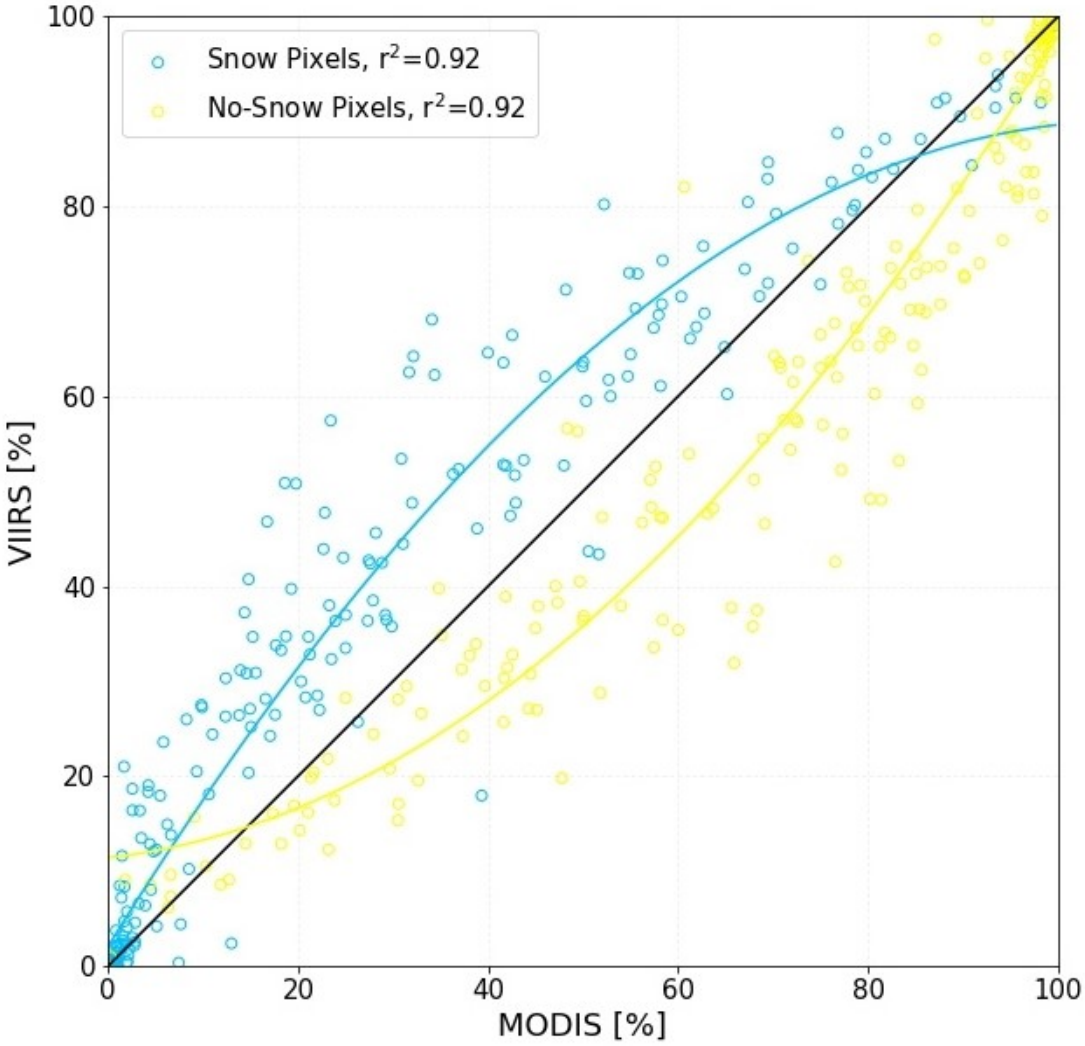

Fig. 9. Scatter plots illustrating VIIRS snow and no-snow pixels with respect to MODIS snow and no-snow pixels, excluding all cloud pixels. The deep sky blue and yellow lines represent a second degree polynomial fit for snow and no-snow pixels, respectively.

4.3 Quantitative Comparison between MODIS and VIIRS Snow Maps

Fig. 10 summarizes the snow and no-snow classification agreement and disagreement between MODIS and VIIRS binary snow maps during each day of the 2016 hydrological year on a pixel by pixel basis. The level of agreement between MODIS and VIIRS snow map is measured by MODIS snow – VIIRS snow and MODIS no-snow – VIIRS no-snow pixels, which are the cases where both MODIS and VIIRS agree on snow-covered and snow-free conditions to the total number of comparisons as recommended by Klein and Barnet, 2003. The MODIS snow – VIIRS snow (blue line) and MODIS no-snow – VIIRS no-snow (yellow line) representation on Fig. 10 also indicates the general timing of the snow and no-snow season over the study area. The major snow season over the study area was during mid-November to mid-April. On the other hand, the level of disagreement between MODIS and VIIRS snow map is measured by MODIS snow – VIIRS no-snow and MODIS no-snow – VIIRS snow pixels which are the cases where either MODIS or VIIRS maps snow but the other does not (Klein and Barnet, 2003). In Fig. 10, the green line is the case where MODIS maps snow but VIIRS does not (omission errors), while the red line no-snow while red line is the case where MODIS maps no-snow but VIIRS maps snow (commission errors). These two line depicts that typically VIIRS maps more snow pixels compared to MODIS even at the 30% NDIS Snow Cover threshold.

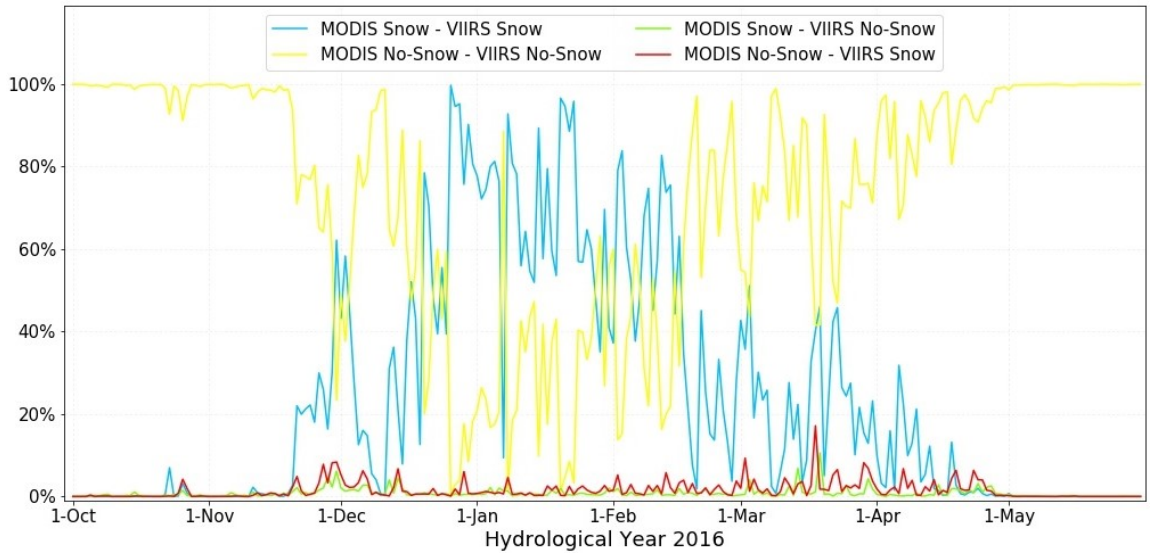

Fig. 10. Line plots illustrating MODIS snow – VIIRS snow agreement, MODIS no-snow – VIIRS no-snow agreement, MODIS snow – VIIRS no-snow omission, and MODIS no-snow – VIIRS snow commission with respect to each day of the 2016 hydrological year.

Table 4 represents the confusion matrix for all non-cloudy pixels mapped during the study period. The first number in the cell indicates total number of pixel counts while the number in parenthesis indicates the percentage of these counts. On average during the study period, about 1% of time MODIS mapped snow but VIIRS did not, whereas 2% of the time VIIRS mapped snow but MODIS did not. So, overall VIIRS is slightly overestimating the snow cover area during the 2016 hydrological year compared to MODIS. The overall agreement between MODIS and VIIRS was about 98% with Cohen's Kappa 0.601, indicating moderate level of agreement according to Landis and Koch (1977). Fig. 11 illustrates pattern of overall agreement and Kappa statistics during each day of the 2016 hydrological year over the study area.

Table 4. Confusion matrix between MYD10L2 and VSCMO during the 2016 hydrological year

		MODIS	
		Snow	No snow
VIIRS	Snow	719307.73 (24.08%)	55370.78 (1.53%)
	No snow	28203.70 (0.80%)	3604280.79 (73.59%)
		Overall agreement: 97.67%, K_{hat}: 0.601	

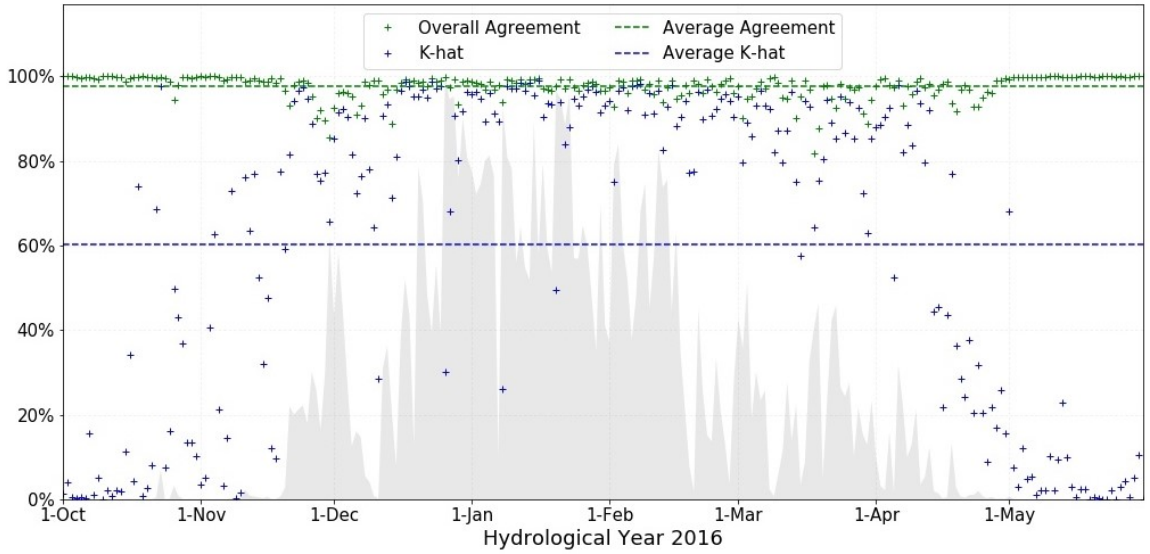

Fig. 11. Marker plots showing Overall Agreement and Kappa statistics between MODIS and VIIRS snow maps with respect to each day of the 2016 hydrological year. The green and blue dash lines respectively represent the average overall agreement (97.67%) and average Kappa statistics (0.601) between MODIS and VIIRS snow maps. The gray area represents the percentage of cells mapped by both MODIS and VIIRS as snow each day.

In the analysis, when either the agreement between MODIS and VIIRS for snow or non-snow become small, approximately 5% of the total pixels, the Kappa statistics become unreliable estimates of the agreement between the two snow products. This is more typically a problem in the snow-free season when few snow covered pixels occur. Tables 5 and 6 provide two good examples of the problem.

Table 5. Confusion matrix between MYD10L2 and VSCMO during Nov. 18, 2015

		MODIS	
		Snow	No snow
VIIRS	Snow	305 (0.08%)	2180 (0.60%)
	No snow	3055 (0.84%)	358661 (98.48%)
		Overall agreement: 98.56%, K_{hat}: 0.097	

Table 6. Confusion matrix between MYD10L2 and VSCMO during Jan. 8, 2015

		MODIS	
		Snow	No snow
VIIRS	Snow	318721 (92.80%)	15944 (4.64%)
	No snow	4643 (1.35%)	4129 (1.20%)
		Overall agreement: 94.01%, K_{hat}: 0.260	

Thus, all data with MODIS snow – VIIRS snow or MODIS no-snow – VIIRS no-snow value less than 5% were removed and reanalyzed. Table 7 and Fig. 12 is an example demonstrating an improvement on the Cohen's Kappa with 0.899 indicating almost perfect level of agreement according to Landis and Koch (1977).

Table 7. Average confusion matrix between MYD10L2 and VSCMO

		MODIS	
		Snow	No snow
VIIRS	Snow	1238750.13 (39.92%)	79840.82 (2.35%)
	No snow	36895.04 (1.14%)	2145007.33 (56.59%)
		Overall agreement: 96.51%, K_{hat}: 0.899	

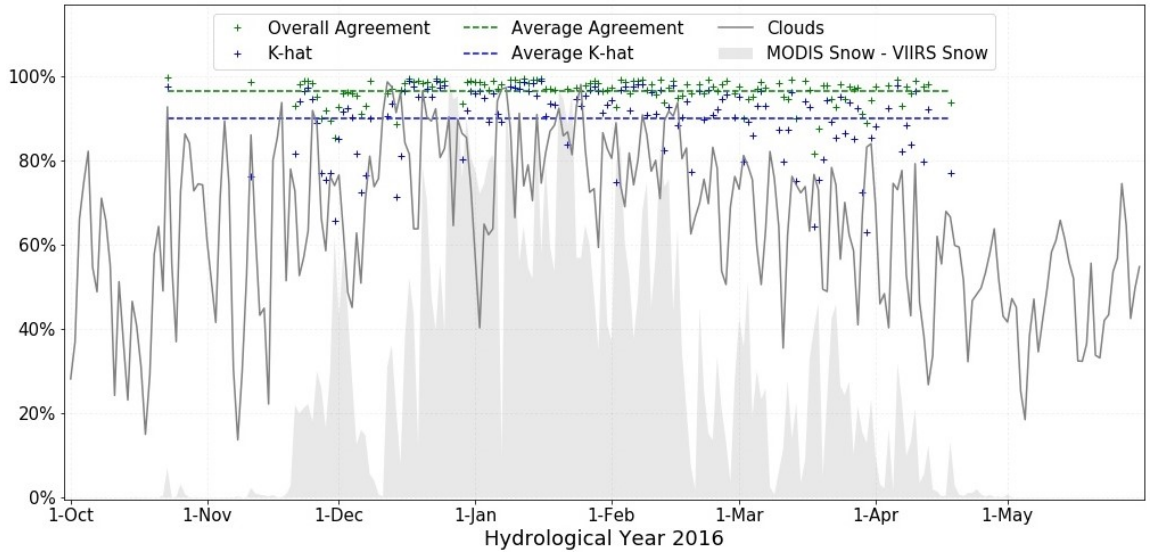

Fig. 12. Marker plots showing improvement in Kappa statistics between MODIS and VIIRS snow maps with respect to each day of the 2016 hydrological year. The green and blue dash lines respectively represent the average overall agreement (96.51%) and average kappa statistics (0.899) between MODIS and VIIRS snow maps.

Tables 8, 9, 10 & 11 demonstrate the examples of confusion matrix between MODIS and VIIRS snow maps showing moderate level of Kappa statistics, while Tables 12, 13, 14 & 15 demonstrate the examples of confusion matrix for individual days showing almost perfect level of Kappa statistics.

Table 8. Confusion matrix between MYD10L2 and VSCMO during Nov. 27, 2015

		MODIS	
		Snow	No snow
VIIRS	Snow	1244937 (25.98%)	374992 (7.82%)
	No snow	98955 (2.06%)	3073387 (64.13%)
		Overall agreement: 90.11%, K_{hat}: 0.769	

Table 9. Confusion matrix between MYD10L2 and VSCMO during Nov. 30, 2015

		MODIS	
		Snow	No snow
VIIRS	Snow	1882374 (62.16%)	253431 (8.37%)
	No snow	186922 (6.17%)	705651 (23.30)
		Overall agreement: 85.46%, K_{hat}: 0.658	

Table 10. Confusion matrix between MYD10L2 and VSCMO during Dec. 14, 2015

		MODIS	
		Snow	No snow
VIIRS	Snow	239887 (21.01%)	76844 (6.73%)
	No snow	51142 (4.48%)	773857 (67.78%)
		Overall agreement: 88.79%, K_{hat}: 0.713	

Table 11. Confusion matrix between MYD10L2 and VSCMO during Mar 18, 2016

		MODIS	
		Snow	No snow
VIIRS	Snow	1134148 (40.20%)	483929 (17.15%)
	No snow	31605 (1.12%)	1171779 (41.53%)
		Overall agreement: 81.73%, K_{hat}: 0.644	

Table 12. Confusion matrix between MYD10L2 and VSCMO during Dec. 24, 2015

		MODIS	
		Snow	No snow
VIIRS	Snow	1319549 (55.52%)	16392 (0.69%)
	No snow	16468 (0.69%)	1024452 (43.10%)
		Overall agreement: 98.62%, K_{hat}: 0.972	

Table 13. Confusion matrix between MYD10L2 and VSCMO during Jan. 10, 2016

		MODIS	
		Snow	No snow
VIIRS	Snow	3995997 (78.22%)	15964 (0.31%)
	No snow	31230 (0.61%)	1065618 (20.86%)
		Overall agreement: 99.08%, K_{hat}: 0.973	

Table 14. Confusion matrix between MYD10L2 and VSCMO during Jan. 16, 2016

		MODIS	
		Snow	No snow
VIIRS	Snow	2180045 (57.70%)	10812 (0.29%)
	No snow	8920 (0.24%)	1578575 (41.78%)
		Overall agreement: 99.48%, K_{hat}: 0.989	

Table 15. Confusion matrix between MYD10L2 and VSCMO during Feb. 4, 2016

		MODIS	
		Snow	No snow
VIIRS	Snow	2586128 (60.41%)	40335(0.94%)
	No snow	11271 (0.26%)	1643525 (38.39%)
		Overall agreement: 98.79%, K_{hat}: 0.975	

4.4 Qualitative Comparison with False Color Composite Imagery

The false color imagery of both MODIS and VIIRS were compared with their corresponding snow maps. Figs. 13, 14, 15, 16 & 17 are the example of the visual comparison of MODIS and VIIRS snow maps with their respective false color images at different dates. The visual comparison depicts good qualitative agreement between snow cover area visible in MODIS and VIIRS false color images (blue hue) and mapped in their respective snow cover products. The false color comparison between MODIS and VIIRS demonstrates that snow cover area is slightly higher in VIIRS compared to MODIS while cloud cover portion is higher in MODIS, which could be associated with different cloud cover mask used for MODIS and VIIRS snow cover product. Figs. 13 & 14 exhibits more area mapped as snow in VIIRS compared to MODIS. Also, snow/cloud confusion over the traces of snow, particularly in snow/no-snow transition zone is higher in MODIS as compared to VIIRS as depicted in Figs. 15 & 16, which could be the reason for higher VIIRS snow commission.

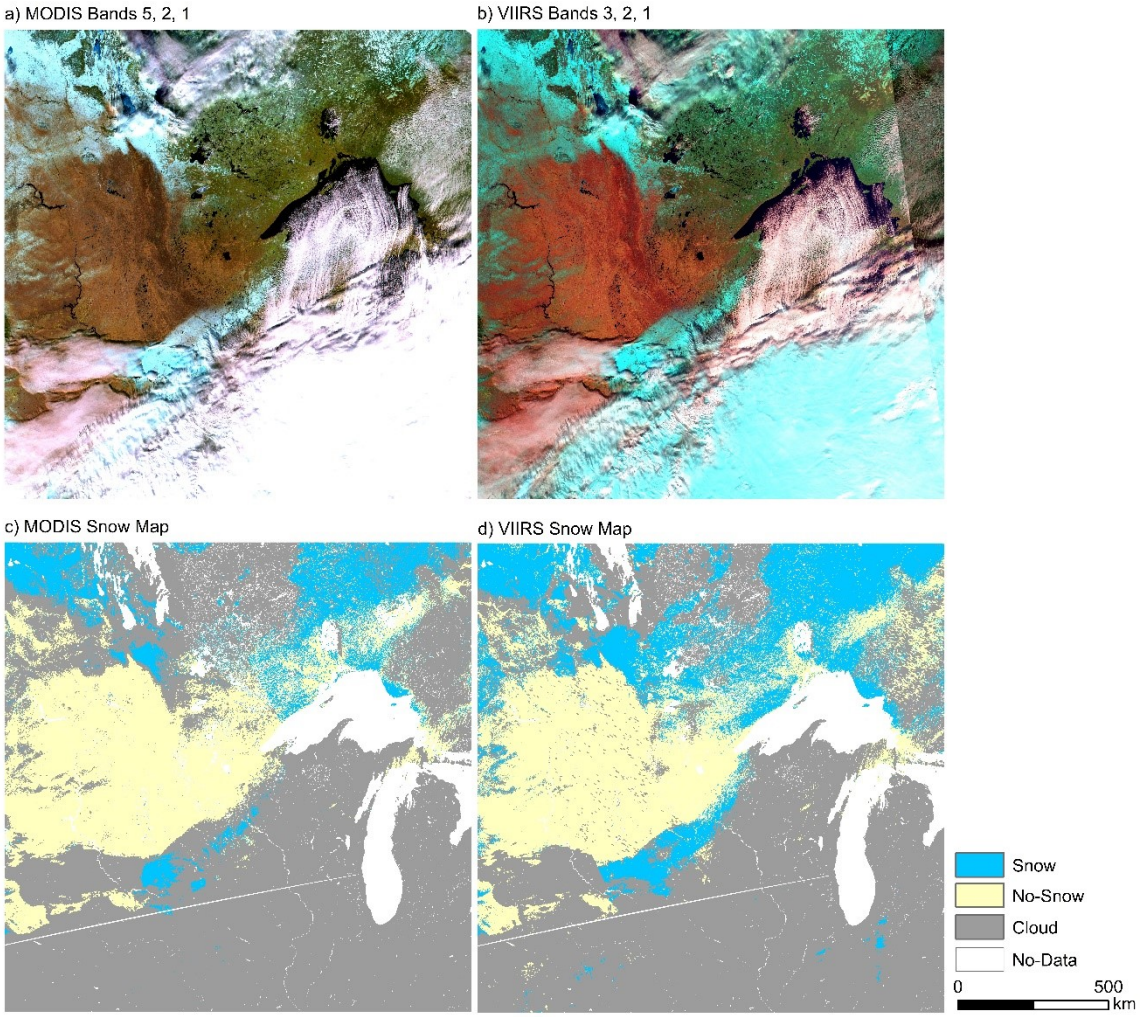

Fig. 13. Qualitative comparison during Nov 27, 2015. (a) A false-color composite image of MODIS bands 5, 2, 1 as R, G and B that shows snow as cyan color; (b) a false-color composite image of VIIRS bands 3, 2, 1 as R, G and B that shows snow as cyan color; (c) MODIS binary snow map and (d) VIIRS binary snow map.

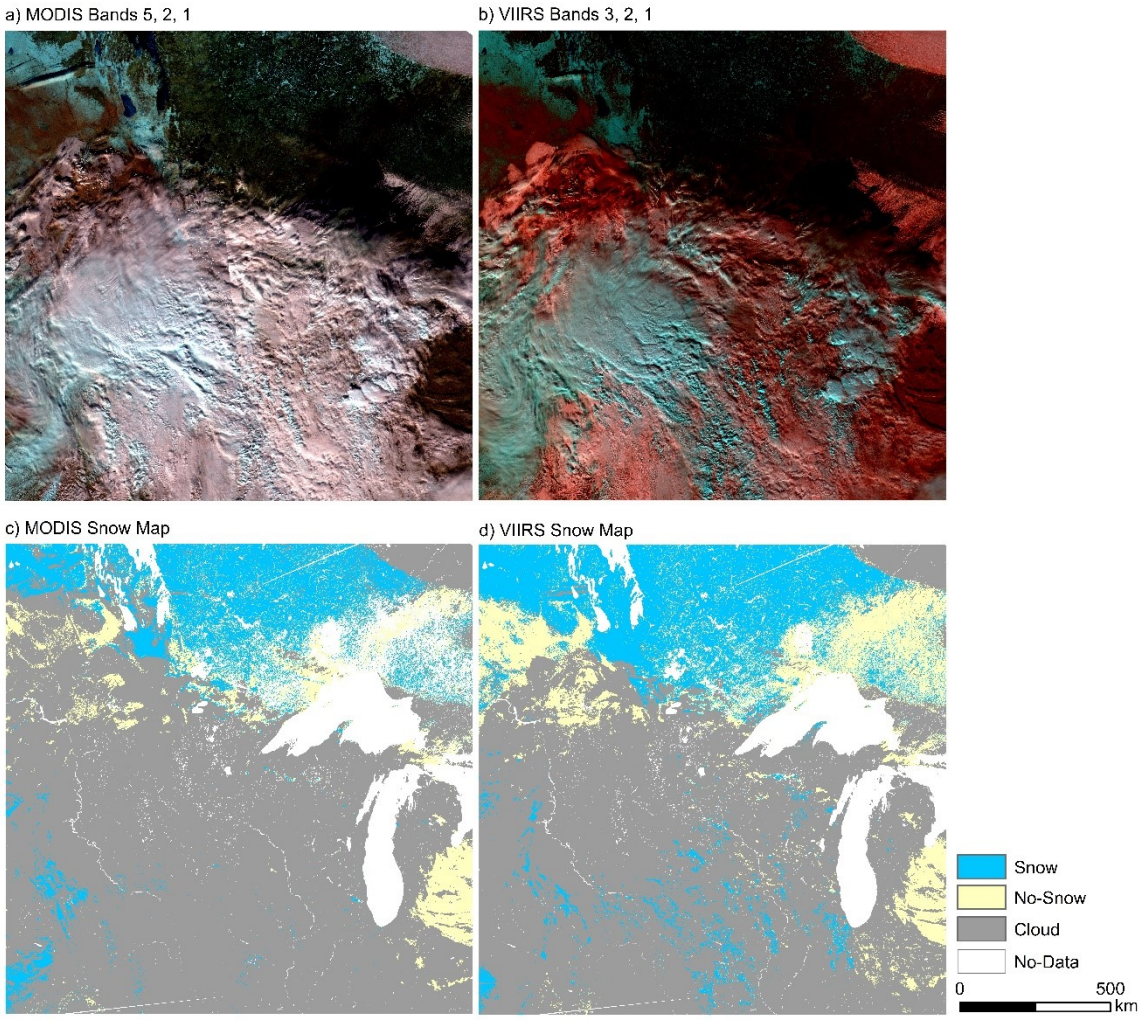

Fig. 14. Qualitative comparison during Nov 30, 2015. (a) A false-color composite image of MODIS bands 5, 2, 1 as R, G and B that shows snow as cyan color; (b) a false-color composite image of VIIRS bands 3, 2, 1 as R, G and B that shows snow as cyan color; (c) MODIS binary snow map and (d) VIIRS binary snow map.

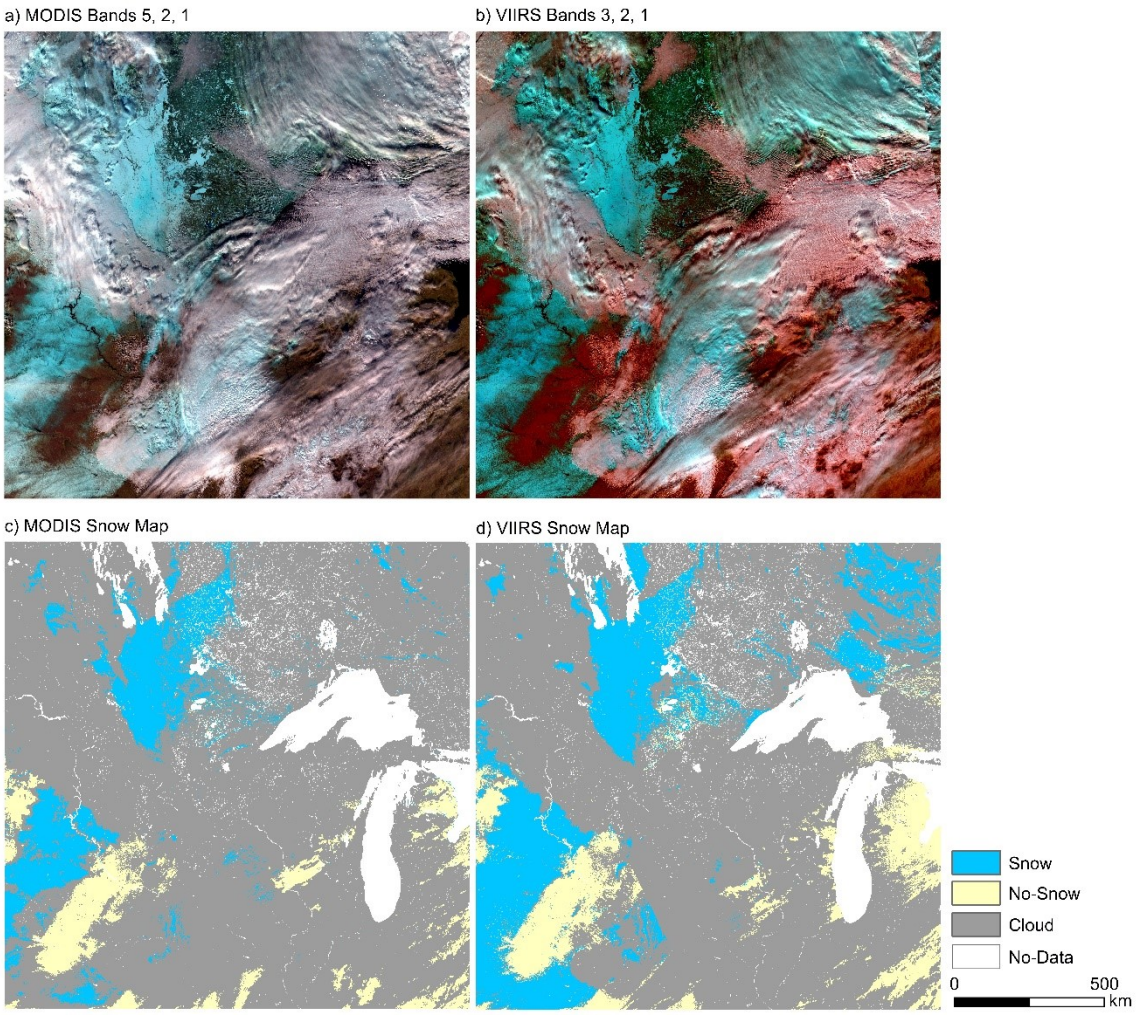

Fig. 15. Qualitative comparison during Dec 24, 2015. (a) A false-color composite image of MODIS bands 5, 2, 1 as R, G and B that shows snow as cyan colors; (b) a false-color composite image of VIIRS bands 3, 2, 1 as R, G and B that shows snow as cyan colors; (c) MODIS binary snow map and (d) VIIRS binary snow map.

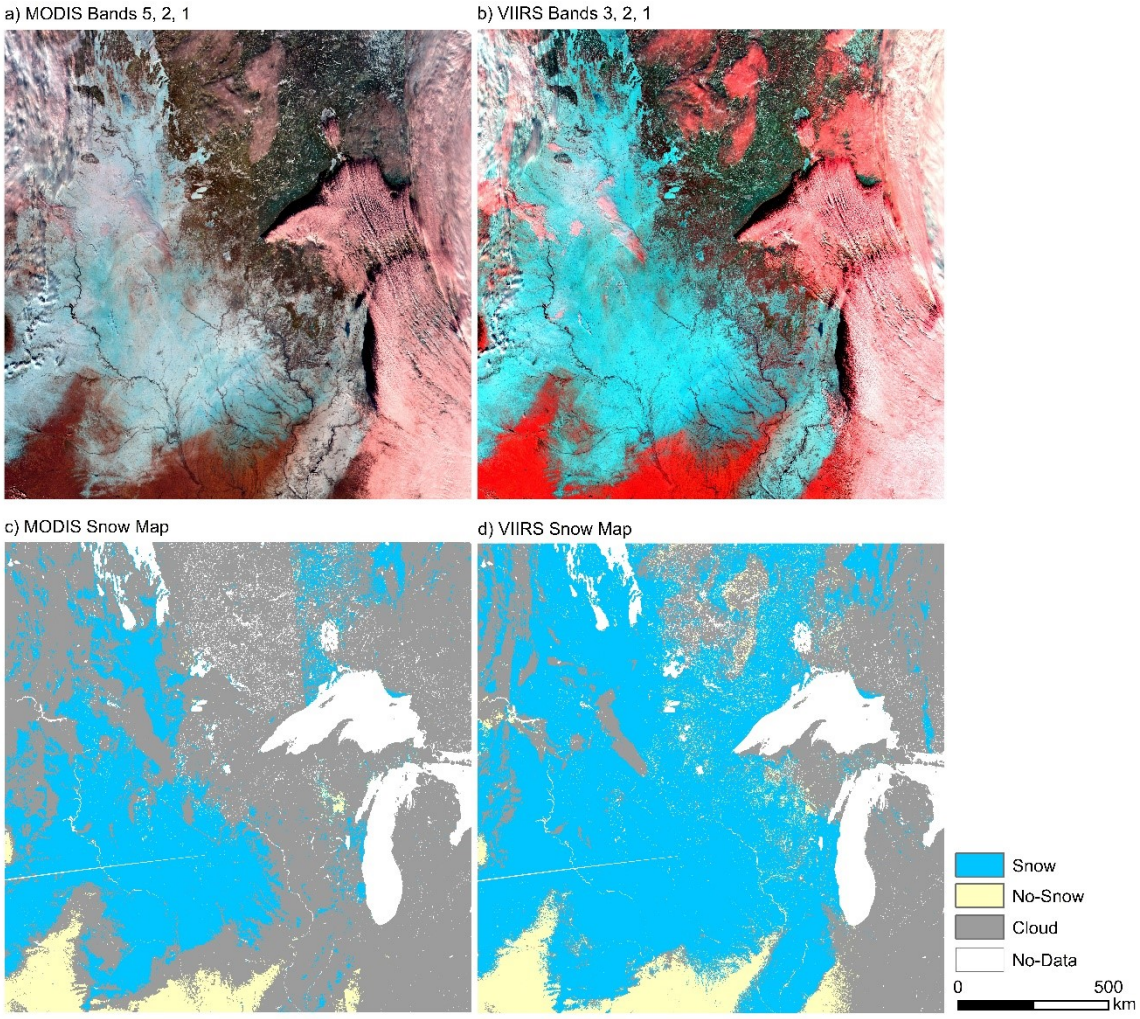

Fig. 16. Qualitative comparison during Jan 10, 2016. (a) A false-color composite image of MODIS bands 5, 2, 1 as R, G and B that shows snow as cyan colors; (b) a false-color composite image of VIIRS bands 3, 2, 1 as R, G and B that shows snow as cyan colors; (c) MODIS binary snow map and (d) VIIRS binary snow map.

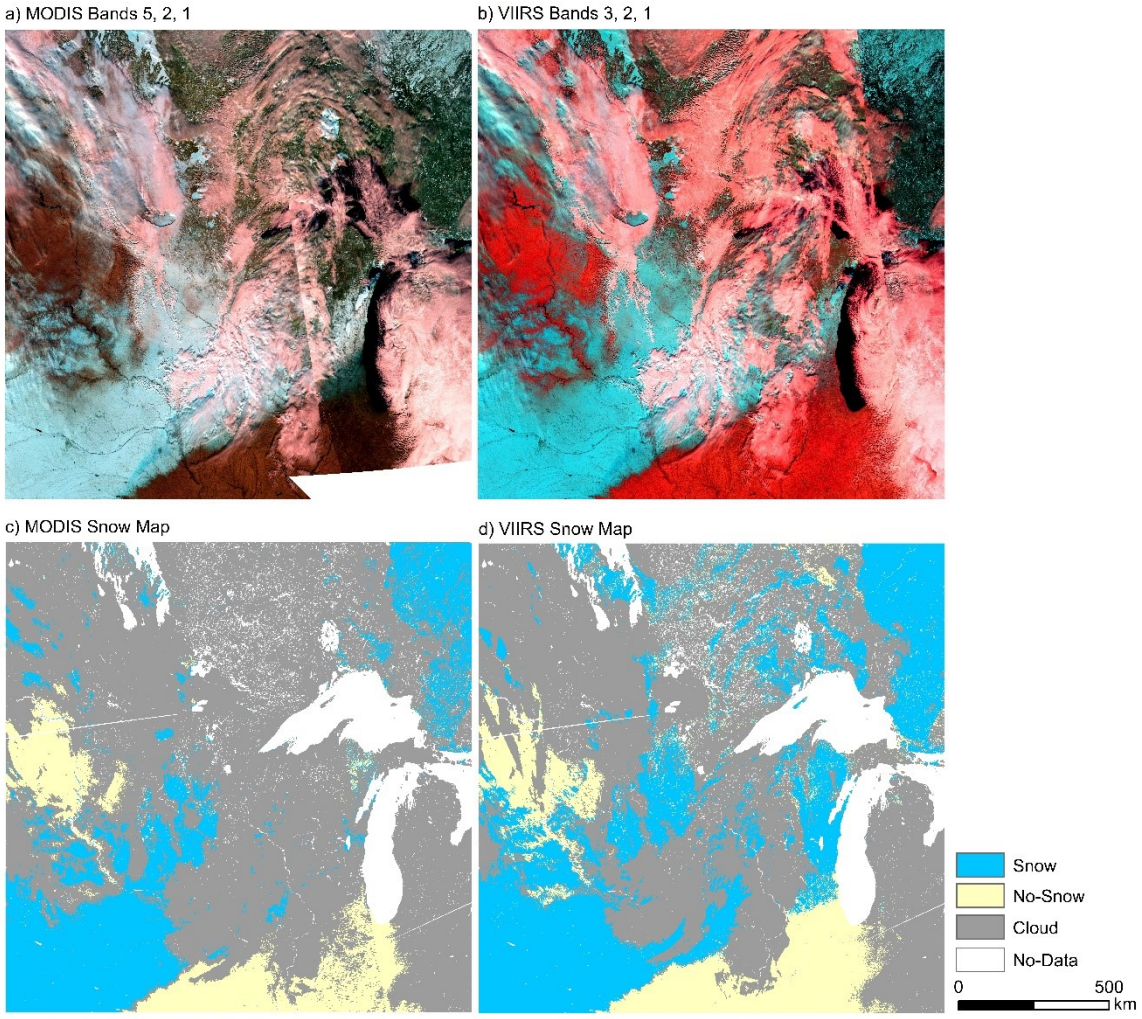

Fig. 17. Qualitative comparison during Feb 4, 2016. (a) A false-color composite image of MODIS bands 5, 2, 1 as R, G and B that shows snow as cyan colors; (b) a false-color composite image of VIIRS bands 3, 2, 1 as R, G and B that shows snow as cyan colors; (c) MODIS binary snow map and (d) VIIRS binary snow map.

4.5 Qualitative Comparison for Individual Days

Comparison maps for individual days were developed for the better assessment of snow mapping differences between MODIS and VIIRS (Klein and Barnet, 2003). The visual assessment of the comparison maps indicates that the overall agreement between MODIS and VIIRS is high during the winter season. Similarly, the disagreement between MODIS and VIIRS snow is high during late fall or early winter, mostly over the dense forest area (Figs. 18 & 19). Additionally Figs. 20 & 21 depicts that MODIS has mapped more clouds as compared to VIIRS, particularly over the edges of snow covered areas. Furthermore, snow/no-snow transition zone is mapped as clouds in both MODIS and VIIRS (Fig. 22).

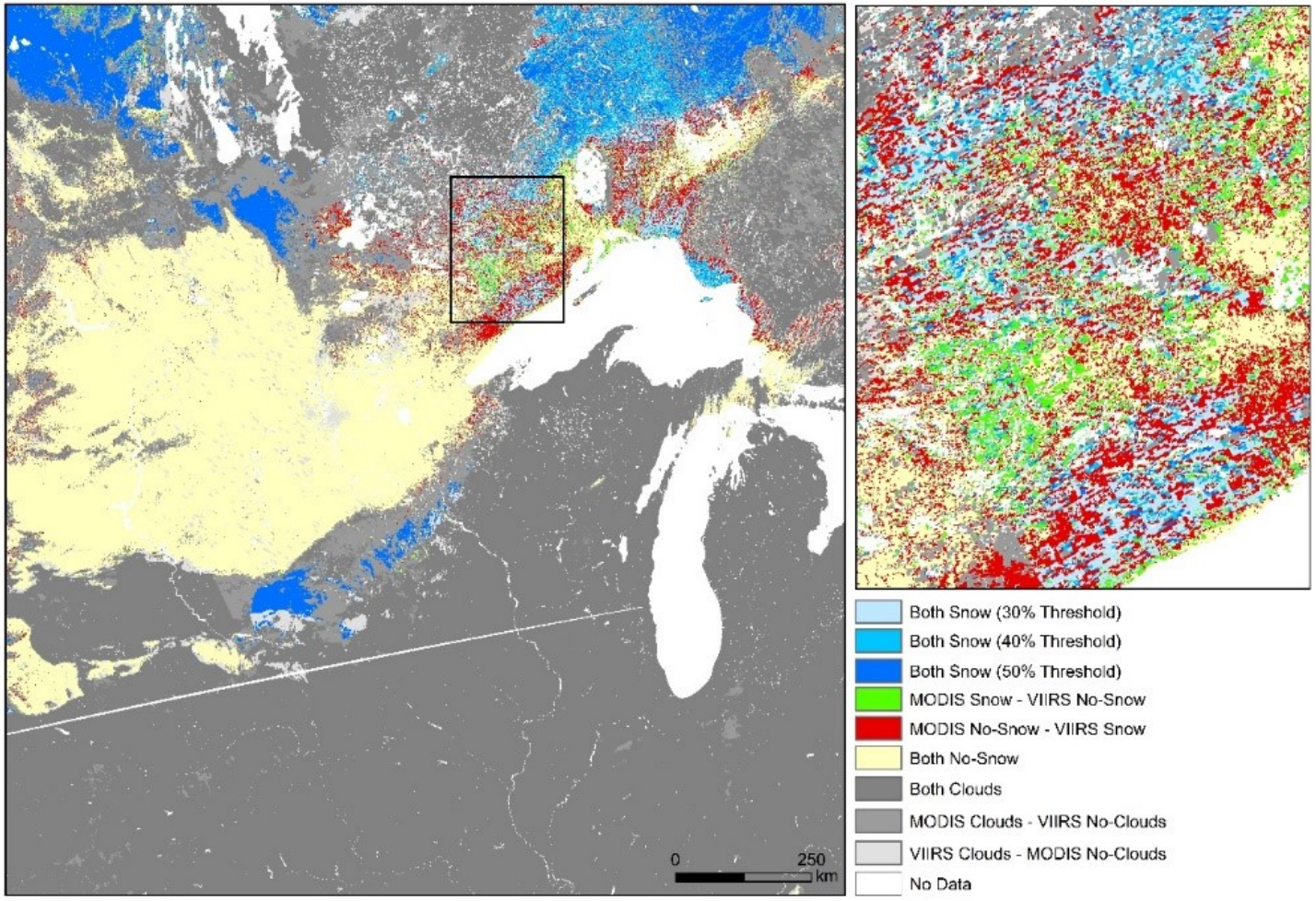

Fig. 18. MODIS and VIIRS snow comparison map for November 27, 2015 illustrating disagreement over forest areas.

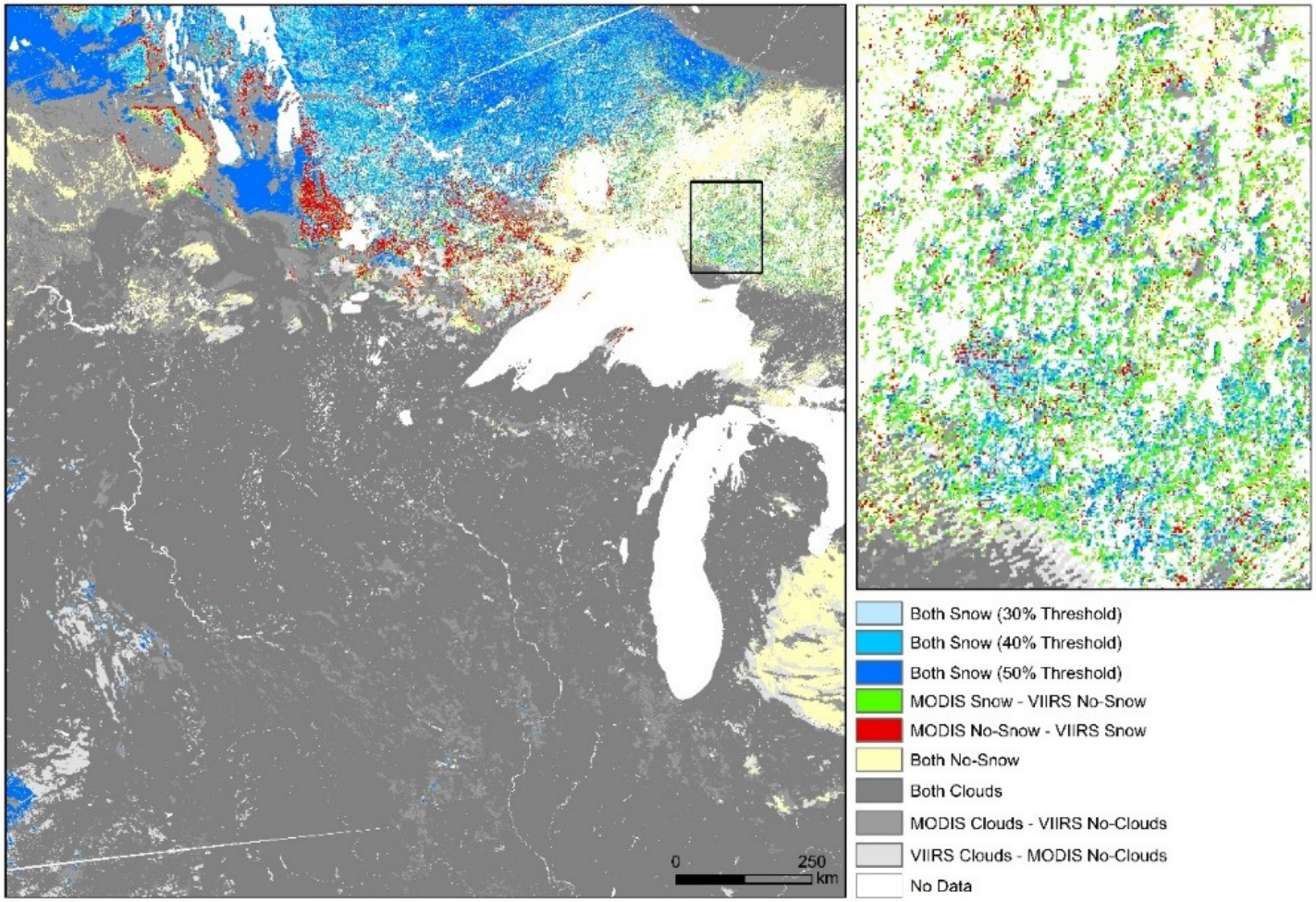

Fig. 19. MODIS and VIIRS snow comparison map for November 30, 2015 illustrating disagreement over forest areas.

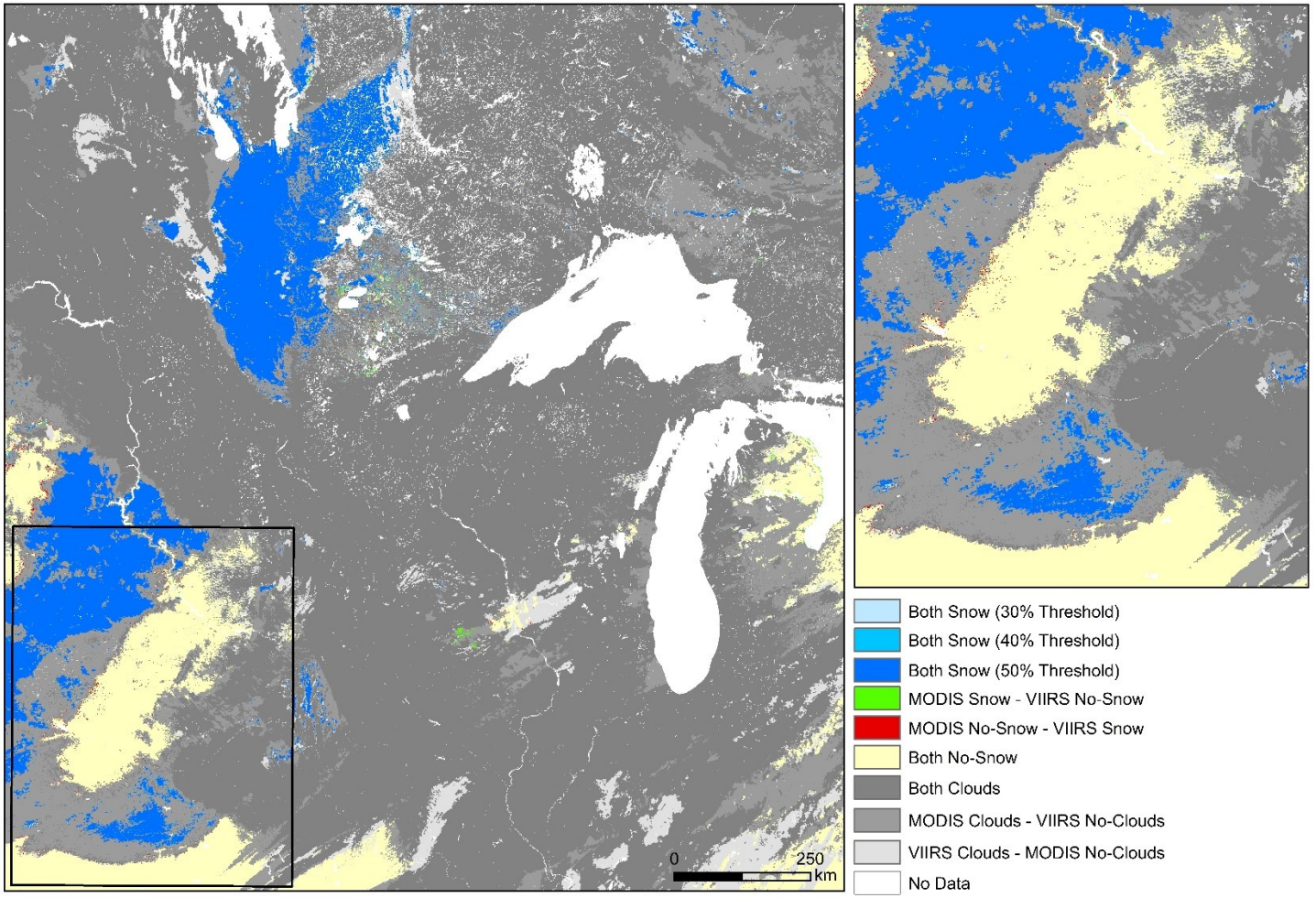

Fig. 20. MODIS and VIIRS snow comparison map for December 24, 2015 illustrating disagreement over snow/no-snow transition zone where MODIS mapped cloud but VIIRS did not.

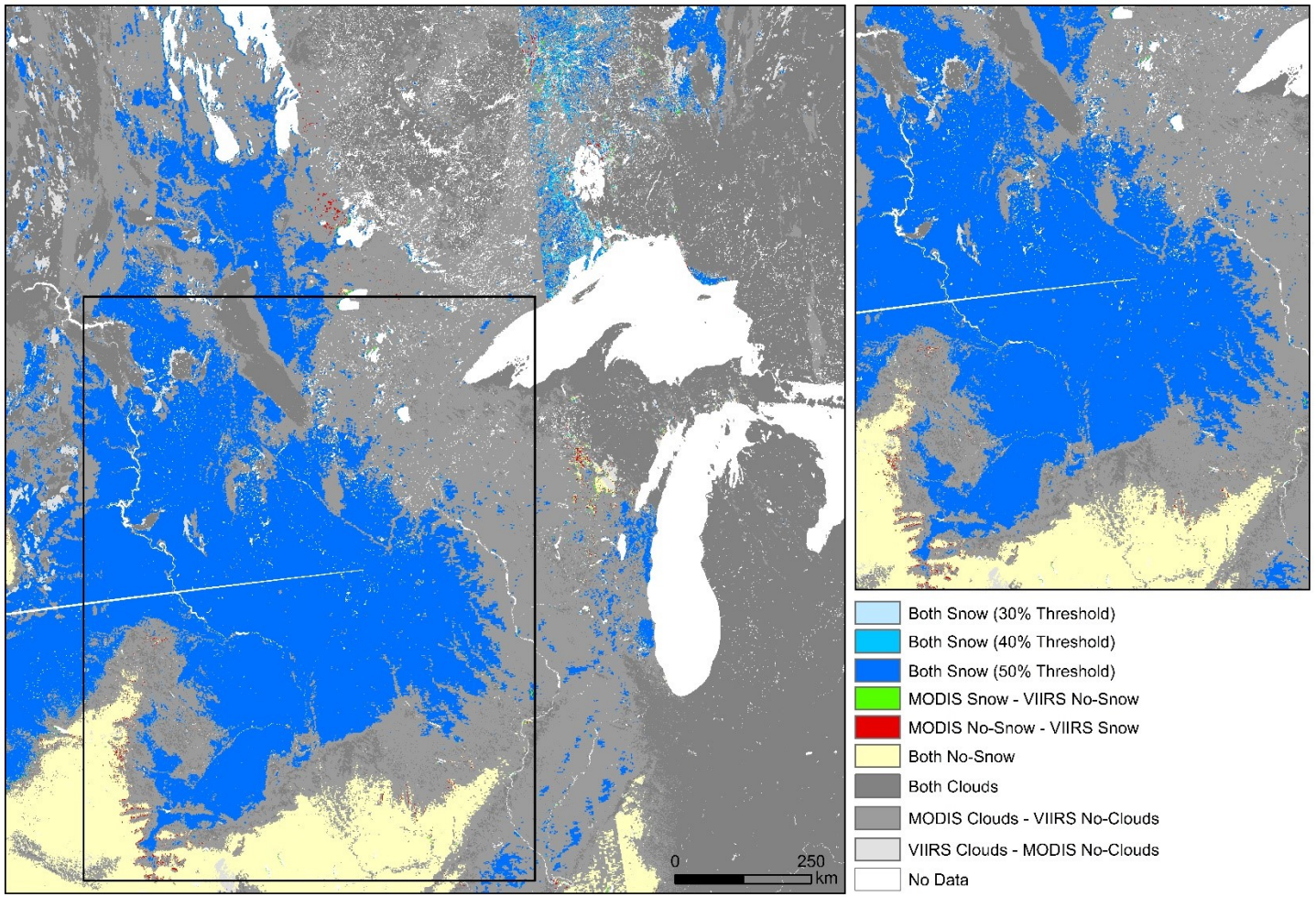

Fig. 21. MODIS and VIIRS snow comparison map for January 10, 2016 illustrating MODIS mapped more clouds than VIIRS.

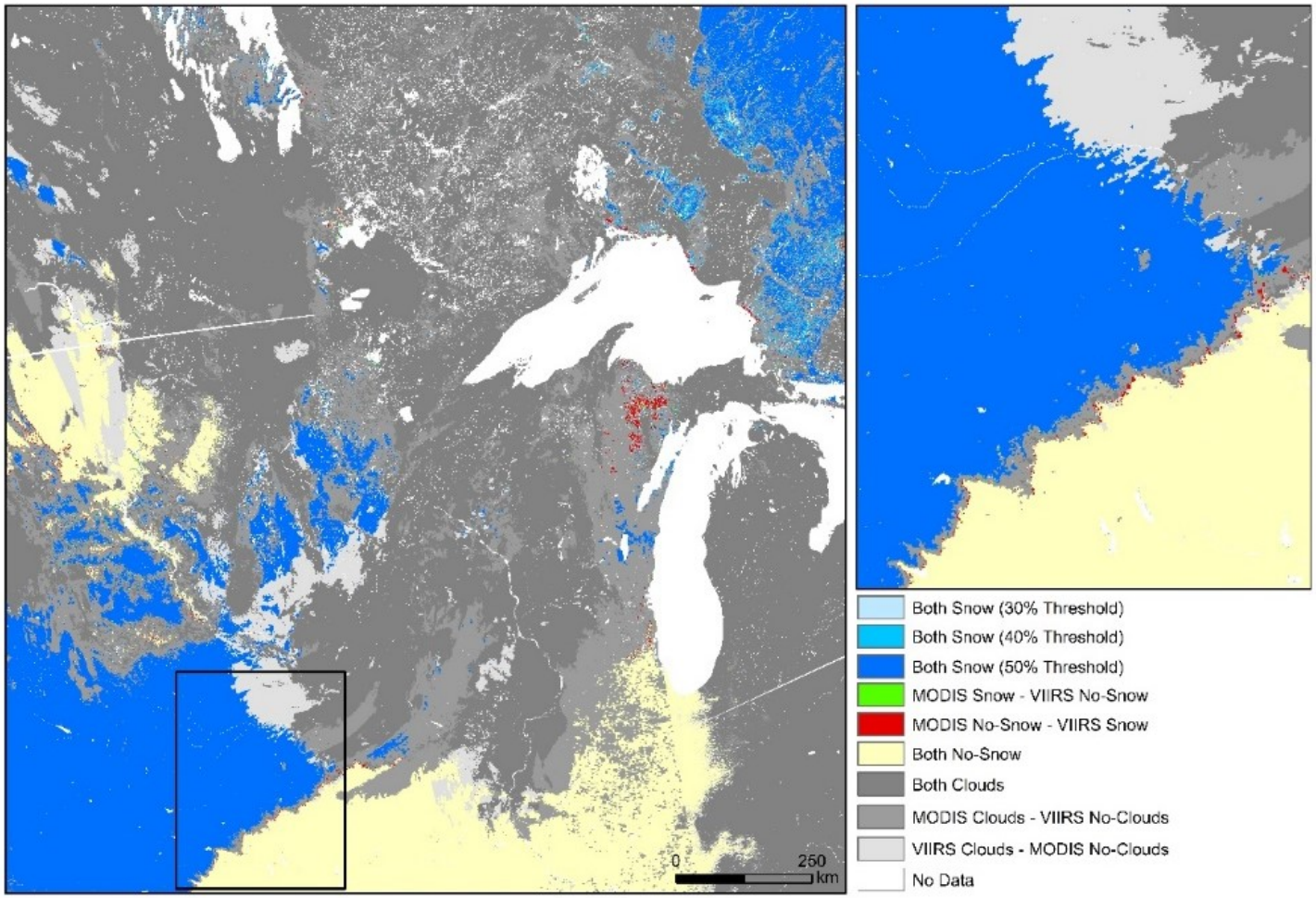

Fig. 22. MODIS and VIIRS snow comparison map for February 4, 2016 illustrating snow/no-snow transition zone mapped as clouds.

5. DISCUSSION

5.1 MODIS Fractional Snow Cover Threshold

The optimal fractional snow cover threshold of the MODIS swath snow map was determined as 30% to generate MODIS binary snow cover maps most comparable to the VIIRS products over the study area. Prior to MODIS C6 snow products, NDSI threshold value of 0.4 recommended by Dozier 1989 was used to produce MODIS binary snow map. However, this value is not universally applicable (Solberg, 2006) and binary map was deleted in MODIS Collection 6 where snow cover area is represented as NDSI Snow Cover in the range of 0-100% (Riggs et al., 2016a). User can select the NDSI threshold for snow using the NDSI Snow Cover based on land cover types of the study area to produce binary snow maps (Riggs et al., 2016a).

The NDSI threshold of 0.4 is equivalent to 50% or more snow cover fraction in a pixel (Hall et al., 2001), and VIIRS binary snow map is limited to an NDSI range of 0.4 to 1.0 (Baker, 2011; Justice et al., 2013). However, in this study, when MODIS binary snow map generated at 50% FSC threshold was compared with VIIRS snow map, average snow omission for MODIS was high around 45%. However, the snow omission decreases with the decrease in threshold values and at nearly 30% threshold value, snow omission error for both MODIS and VIIRS was equivalent. Consequently, 30% FSC value was used as a threshold to produce MODIS binary snow maps. Thus, 0.4 NDSI threshold is not applicable to produce MODIS binary snow maps most comparable to VIIRS binary snow map over the study area.

VIIRS is considered as an extension of MODIS (Zhang et al., 2016). In order to ensure the smooth transition of MODIS to VIIRS in climate data records developed from both satellites, snow cover extent needs to be comparable between MODIS and VIIRS. The higher spatial resolution of VIIRS potentially enables it to map snow cover area more accurately than MODIS. This study suggest that VIIRS is slightly overestimating (6% more) the snow when compared to MODIS at the 30% FSC threshold which appears to produce the most comparable snow cover maps. However, VIIRS snow commission errors relative to MODIS increase with increases in MODIS FSC thresholds, which could mislead that snow cover is increasing once VIIRS replaces MODIS. Thus, 50% MODIS FSC threshold does not best approximates the VIIRS binary snow product in this study.

5.2 Total Snow, No-Snow and Cloud

On average, MODIS and VIIRS snow map classified comparable areas as no-snow pixels. However, VIIRS categorized fewer pixels (5% less on average) as cloud compared to MODIS. Key et al. (2013) depicted that the fraction of cloud pixels in VIIRS binary snow map was 65-70% during a six month period running from December 2012 to May 2013. However, this study exhibited 59.91% as the average cloud pixel in VIIRS during the study period of the 2016 hydrological year. This difference could be due to the improvement in the VIIRS Cloud Mask algorithm. Similarly, this study depicted 65.02% as the cloud pixel in MODIS which is within the range of 65-70% illustrated by Wang et al. (2009) in collection 4 MODIS snow products. Although the

cloud mask used for MODIS C6 snow cover product have been revised, it has not been able to reduce cloud/snow confusion completely (Riggs et al., 2016a), which is also present in VIIRS snow products. Thus, cloud is a major limiting factor in optical snow cover mapping.

The average aerial coverage of snow pixels is 5.72% and 11.43% of total area in MODIS and VIIRS snow cover maps, respectively. Thus, VIIRS classified almost 6% more of the study area snow compared to MODIS. These differences were more prevalent during the winter and spring season. The variances in snow and cloud pixels between MODIS and VIIRS could be associated with the differences in MODIS and VIIRS cloud mask.

5.3 Quantitative Comparison between MODIS and VIIRS Snow Maps

The quantitative intercomparison between MODIS and VIIRS snow cover map indicates good agreement between them with 97.67% average agreement during the 2016 hydrological year. Thus, VIIRS has the potential of providing continuity to binary MODIS snow products. The agreement between MODIS and VIIRS snow map is higher during winter season than during late fall or spring season. For example, on 17th Dec. 2015, the overall agreement was 99.40% with Kappa statistics 0.988 indicating almost perfect level of agreement according to Landis and Koch (1977). However, during early spring on 18th Mar. 2016 when snow cover is patchy, the overall agreement between MODIS and VIIRS decreases to 81.73% with Kappa statistics 0.644 indicating moderate

level of agreement. Similar results was observed by Ault et al. (2006) and Key et al. (2013) in their studies of MODIS and VIIRS snow cover products.

Many factors affect the agreement between MODIS and VIIRS snow maps. One of the potentially important factors are errors associated with the preprocessing steps including data projection and resampling (Lunetta et al., 1991). In this study, 500 m MODIS was oversampled to 375 m for MODIS-VIIRS binary comparison. Additionally, the 250 m water mask was undersampled to 375 m before extracting the land pixels. In addition, Differences in spatial and spectral resolution between MODIS and VIIRS could influence their agreement.

5.4 Qualitative Comparison with False Color Composite Imagery

The visual comparison of MODIS and VIIRS with their corresponding false color imagery exhibited good agreement with the major patterns of the snow cover distribution. Some irregularities were observed in forested areas during early spring that could be associated with low reflectance of aged melting snow in the visible spectral bands (Key et al., 2013). VIIRS tends to map more snow in forest areas than MODIS. The false color imagery of MODIS and VIIRS also exhibit that snow cover area represented by blue hue is more visible and clearer in VIIRS that could be due to higher spatial resolution of VIIRS. Moreover, comparison of false color imagery with the snow cover map reveals that MODIS cloud mask tends to map more areas as cloudy as compared to VIIRS, specifically along the snow/no-snow transition zone and when snow

cover is patchy. However, snow/cloud confusion is prevalent in both MODIS and VIIRS snow maps.

5.5 Qualitative Comparison for Individual Days

To assess the differences in snow mapping between MODIS and VIIRS, comparison maps for individual days during the 2016 hydrological year was produced (Klein and Barnet, 2003). The comparison maps exhibited that snow classification disagreement between MODIS and VIIRS tends to be higher in mixed forest areas, whereas the agreement is higher in the areas with limited or non-dense vegetation such as grasslands and croplands. Hall and Riggs (2007) also reported higher accuracy up to 99% in croplands and agricultural areas, and lower accuracy in evergreen forest of MODIS snow product, particularly during early snow season and snow melt season. VIIRS is mapping more snow in forest areas than MODIS. This could be due to the lower spatial resolution of MODIS compared to VIIRS.

Similarly, both MODIS and VIIRS snow map recorded the boundaries of the snow-covered areas or the snow/land transition zone as cloudy. MODIS cloud mask is more likely to map the boundaries of snow-covered areas as cloudy as depicted by Ault et al., 2006 and Wang et al., 2009. Snow/cloud confusion in the land-snow transition is due to thin, sparse or lower fraction of snow on the edges (Klein and Barnet, 2003; Ault et al., 2006; Hall and Riggs, 2007; Wang et al., 2009). The cloud mask often identifies thin, sparse snow cover as cloud because snow may not cover a large percentage pixel to exhibit strong spectral signature when trace amounts of snow are present, which is more

common on the edge of snow-covered area (Hall and Riggs, 2007). Key et al. (2013) also reported that even during the clear atmosphere, the transition zone between snow and land is often recorded as cloudy in the VIIRS snow map, and they concluded that conservative VIIRS cloud mask was one of the reasons for the snow/cloud confusion. The comparison maps also exhibit that MODIS tends to map more clouds in transition zone as compared to VIIRS.

Snow melt condition, snow cover patchiness or shallow snow depth and vegetation cover visible in the traces of snow also affects the accuracy of snow cover mapping (Ault et al., 2006; Hall and Riggs, 2007). Furthermore, the cloud mask more often likely to mask more clouds than are actually present and sometimes it does not identify certain cloud as cloud (Hall and Riggs, 2007). For example, cirrus cloud is often mapped as snow (Ault et al., 2006).

6. CONCLUSIONS

The analysis and intercomparison of 244 MODIS and VIIRS swath snow maps during the 2016 hydrological year exhibited good overall agreement between them. Furthermore, MODIS NDSI Snow Cover threshold of 30% was determined as optimal for generating MODIS binary snow maps most comparable to VIIRS binary snow maps over the study area. However, this value cannot be generalized beyond this study area. Additionally, the assessment of total snow and cloud pixels and comparison snow maps of MODIS and VIIRS indicates that VIIRS is mapping more snow cover and less cloud cover compared to MODIS. This could be associated with VIIRS being higher spatial resolution (375 m) and dissimilarities in MODIS and VIIRS cloud masks. The overall agreement of 97.67% between MODIS and VIIRS exceeds the VIIRS accuracy requirements of 90% probability of correct typing. From the overall assessment, it can be concluded that VIIRS and MODIS have similar capacity to map snow cover. Moreover, VIIRS has more potential to accurately map snow cover area. Additionally, VIIRS can fulfill the aim of providing long-term continuity of satellite snow cover maps for the successive development of a climate-data record.

VIIRS snow cover map is produced by the NOAA and NASA using different algorithm. Therefore, it is equally important to validate and intercompare NOAA VIIRS and NASA VIIRS snow cover products for their applicability when NASA VIIRS snow map become available to the community. In this study, 500 m spatial resolution of MODIS snow map was oversampled to 375 m to make it comparable with VIIRS snow

map. However, intercomparison studies between MODIS and VIIRS snow products should also consider analysis by undersampling VIIRS snow map to 500 m.

Besides the MODIS – VIIRS snow map intercomparison, it is essential to validate VIIRS snow map using high resolution satellite data such as Landsat and *in situ* snow measurements. Different factors such as time of day, season, and topography should be included in the snow cover validation studies. The validation as well as intercomparison studies should be conducted by different land cover types. Furthermore, detail assessment on the MODIS and VIIRS cloud mask is needed in order to better intercompare MODIS and VIIRS snow maps.

REFERENCES

Ault, T. W., Czajkowski, K. P., Benko, T., Coss, J., Struble, J., Spongberg, A., Templin, M., & Gross, C. (2006). Validation of the MODIS snow product and cloud mask using student and NWS cooperative station observations in the Lower Great Lakes Region. *Remote Sensing of Environment*, *105*, 341-353.

Baker, N. (2011). Joint Polar Satellite System (JPSS) VIIRS Snow Cover Algorithm Theoretical Basis Document (ATBD). Northrop Grumman Aerospace Systems, Redondo Beach, California.

Bunting, J. T., & d'Entremont, R. P. (1982). Detecting cloud phase and snow cover using near infrared satellite measurements. In a conference on Remote Sensing and Atmosphere, Liverpool, 15–17 December 1982. The Remote Sensing Society.

Butt, M. J., & Bilal, M. (2011). Application of snowmelt runoff model for water resource management. *Hydrological Processes*, *25*, 3735-3747.

Channan, S., Collins, K. & Emanuel, W. R. (2014). Global mosaics of the standard MODIS land cover type data. University of Maryland and the Pacific Northwest National Laboratory, College Park, Maryland, USA.

Cohen, J. (1960). A coefficient of agreement for nominal scales. *Educational and Psychological Measurement*, *20*, 37-46.

Congalton, R. G. (1991). A review of assessing the accuracy of classifications of remotely sensed data. *Remote Sensing of Environment*, *37*, 35-46.

Crane, R. G., & Anderson, M. R. (1984). Satellite Discrimination of Snow Cloud Surfaces. *International Journal of Remote Sensing*, *5*, 213-223.

Deng, J., Huang, X. D., Feng, Q. S., Ma, X. F., & Liang, T. G. (2015). Toward Improved Daily Cloud-Free Fractional Snow Cover Mapping with Multi-Source Remote Sensing Data in China. *Remote Sensing*, *7*, 6986-7006.

Dietz, A. J., Kuenzer, C., Gessner, U., & Dech, S. (2012). Remote sensing of snow - a review of available methods. *International Journal of Remote* Sensing, 33, 4094-4134.

Dobreva, I. D., & Klein, A. G. (2011). Fractional snow cover mapping through artificial neural network analysis of MODIS surface reflectance. *Remote Sensing of Environment*, *115*, 3355-3366.

Dozier, J. (1989). Spectral Signature of Alpine Snow Cover from the Landsat Thematic Mapper. *Remote Sensing of Environment*, *28*, 9-22.

Edwards, A. C., Scalenghe, R., & Freppaz, M. (2007). Changes in the seasonal snow cover of alpine regions and its effect on soil processes: A review. *Quaternary International*, *162,* 172-181.

Friedl, M. A., Sulla-Menashe, D., Tan, B., Schneider, A., Ramankutty, N., Sibley, A. & Huang, X. (2010). MODIS Collection 5 global land cover: Algorithm refinements and characterization of new datasets, 2001-2012, Collection 5.1 IGBP Land Cover, Boston University, Boston, MA, USA.

Hall, D. K., & Riggs, G. A. (2007). Accuracy assessment of the MODIS snow cover products. *Hydrological Processes*, *21*, 1534-1547.

Hall, D. K., Kelly, R. E. J., Riggs, G. A., Chang, A. T. C., & Foster, J. L. (2002). Assessment of the relative accuracy of hemispheric-scale snow-cover maps. *Annals of Glaciology*, *34*, 24-30.

Hall, D. K., Riggs, G. A., & Salomonson, V. V. (1995). Development of methods for mapping global snow cover using moderate resolution imaging spectroradiometer data. *Remote Sensing of Environment*, *54*, 127-140.

Hall, D. K., Solberg, R., & Riggs, G. A. (2002). Validation of satellite snow cover maps in North America and Norway. Proceedings of the 59th Eastern Snow Conference, Stowe, VT, 5-7 June 2002.

Hall, D. K., Riggs, G. A., Foster, J. L., & Kumar, S. V. (2010). Development and evaluation of a cloud-gap-filled MODIS daily snow-cover product. *Remote Sensing of Environment*, *114*, 496-503.

Hall, D. K., Riggs, G. A., Salomonson, V. V., Barton, J., Casey, K., Chien, J., DiGirolamo, N., Klein, A., Powell, H., & Tait, A. (2001). Algorithm theoretical basis document (ATBD) for the MODIS snow and sea ice-mapping algorithms. NASA GSFC, September.

Huang, X. D., Liang, T. G., Zhang, X. T., & Guo, Z. G. (2011). Validation of MODIS snow cover products using Landsat and ground measurements during the 2001-2005 snow seasons over northern Xinjiang, China. *International Journal of Remote Sensing*, *32*, 133-152.

Justice, C. O., Román, M. O., Csiszar, I., Vermote, E. F., Wolfe, R. E., Hook, S. J., Friedl, M., Wang, Z., Schaaf, C. B., Miura, T., Tschudi, M., Riggs, G., Hall, D. K., Lyapustin, A. I., Devadiga, S., Davidson, C., & Masuoka, E. J. (2013). Land and cryosphere products from Suomi NPP VIIRS: Overview and status. *Journal of Geophysical Research: Atmospheres*, *118*, 9753-9765.

Key, J. R., Mahoney, R., Liu, Y., Romanov, P., Tschudi, M., Appel, I., Maslanik, J., Baldwin, D., Wang, X., & Meade, P. (2013). Snow and ice products from Suomi NPP VIIRS. *Journal of Geophysical Research: Atmospheres*, *118*, 12816-12830.

Klein, A. G., & Barnett, A. C. (2003). Validation of daily MODIS snow cover maps of the Upper Rio Grande River Basin for the 2000-2001 snow year. *Remote Sensing of Environment*, *86*, 162-176.

Klein, A. G., Hall, D. K., & Riggs, G. A. (1998). Improving snow cover mapping in forests through the use of a canopy reflectance model. *Hydrological Processes, 12*, 1723-1744.

Kung, E. C., Bryson, R. A., & Lenschow, O. H. (1964). Study of a continental surface albedo on the basis of flight measurement and structure of the earth's surface cover. *Monthly Weather Review*, *920*, 543-564.

Kunzi, K. F., Patil, S., & Rott, H. (1982). Snow-covered parameters retrieved from NIMBUS-7 SMMR data. *IEEE Transactions on Geoscience and Remote Sensing*, *4*, 452-467.

Landis, J. R., & Koch, G. C. (1977). The measurement of observer agreement for categorical data. *Biometrics*, *33*, 159-174.

Leathers, D. J., & Luff, B. L. (1997). Characteristics of snow cover duration across the northeast United States of America. *International Journal of Climatology*, *17*, 1535-1547.

Lucas, R. M., & Harrison, A. R. (1990). Snow observation by satellite: a review. *Remote Sensing Reviews*, *4*, 285-348.

Lunetta, R. S., Congalton, R. G., Fenstermaker, L. K., Jensen, J. R., McGwire, K. C. & Tinney, L. R. (1991). Remote Sensing and Geographic Information System Data Integration: Error Sources and Research Issues. *Photogrammetric Engineering & Remote Sensing*, *57*, 677-687.

Maurer, E. P., Rhoads, J. D., Dubayah, R. O., & Dennis, P. L. (2003). Evaluation of the Snow-Covered Area Data Product from Modis. *Hydrological Processes*, *17*, 59-71.

Painter, T. H., Rittger, K., McKenzie, C., Slaughter, P., Davis, R. E., & Dozier, J. (2009). Retrieval of subpixel snow covered area, grain size, and albedo from MODIS. *Remote Sensing of Environment*, *113*, 868-879.

Parajka, J., & Blöschl, G. (2006). Validation of MODIS snow cover images over Austria. *Hydrology and Earth System Sciences Discussions*, *3*, 1569-1601.

Rango, A., Martinec, J., Foster, J., & Marks, D. (1983). Resolution in operational remote sensing of snowcover. In Hydrological Applications of Remote Sensing and Remote Data Transmission. Proceedings of the Hamburg Symposium, August, 1983. IAHS publ. No. 145, 371-382.

Reed, B. (2013). Joint Polar Satellite System (JPSS) Operational Algorithm Description (OAD) Document for VIIRS Snow Cover Environmental Data Record (EDR) Software.

Richards, J. A. (1999). *Remote sensing digital image analysis: an introduction*, 3rd Ed., Springer-Verlag.

Riggs, G. A., Hall, D. K. & Roman, M. O. (2015). VIIRS Snow Cover Algorithm Theoretical Basis Document (ATBD), NASA Goddard Space Flight Center, Greenbelt, Maryland, Version 1.0, December.

Riggs, G. A., Hall, D. K. & Roman, M. O. (2016a). MODIS Snow Products Collection 6 User Guide, version 1.0, August.

Riggs, G. A., Hall, D. K. & Roman, M. O. (2016b). NASA S-NPP VIIRS Snow Products Collection 1 User Guide, version 1.0, December.

Rodell, M., & Houser, P. R. (2004). Updating a land surface model with MODIS-derived snow cover. *Journal of Hydrometeorology*, *5*, 1064-1075.

Romanov, P. (2015). Algorithm Theoretical Basis Document: VIIRS Binary Snow Cover Product, NOAA NESDIS, September 2015.

Rosenthal, W., & Dozier, J. (1996). Automated Mapping of Montane Snow Cover at Subpixel Resolution from the Landsat Thematic Mapper. *Water Resources Research*, *32*, 115-130.

Salomonson, V. V., & Appel, I. (2004). Estimating fractional snow cover from MODIS using the normalized difference snow index. *Remote Sensing of Environment*, *89*, 351-360.

Salomonson, V. V., & Appel, I. (2006). Development of the Aqua MODIS NDSI fractional snow cover algorithm and validation results. *IEEE Transactions on Geoscience and Remote Sensing*, *44*, 1747-1756.

Schowengerdt, R. A. (1997). *Remote Sensing, Models and Methods for Image Processing*, 2nd, San Diego, CA, Academic Press.

Solberg, R., & Andersen, T. (1994). An automatic system for operational snow-cover monitoring in the Norwegian mountain regions. Proceedings of IGARSS 1994 symposium, Pasadena, CA, 2084-2086.

Solberg, R., Koren, H. & Amlien, J. (2006). A review of optical snow cover algorithms. Norwegian Computing Center Note, No. SAMBA/40/06.

Vikhamar, D., & Solberg, R. (2003). Subpixel mapping of snow cover in forests by optical remote sensing. *Remote Sensing of Environment*, *84*, 69-82.

Wang, L., Derksen, C., & Brown, R. (2008). Detection of pan-Arctic terrestrial snowmelt from QuickSCAT, 2000–2005. *Remote Sensing of Environment*, *112*, 3794-3805.

Wang, X. W., Xie, H. J., Liang, T. G., & Huang, X. D. (2009). Comparison and validation of MODIS standard and new combination of Terra and Aqua snow cover products in northern Xinjiang, China. *Hydrological Processes*, *23*, 419-429.

Warren, S. G. & Wiscombe, W. J. (1980). A model for the spectral albedo of snow. II: Snow containing atmospheric aerosols. *Journal of Atmospheric Sciences*, *37*, 2735-2745.

White, D. A. (2016a). The MODIS Conversion Toolkit (MCTK) User's Guide. Available online: https://github.com/dawhite/MCTK/releases (accessed on 15 December 2016).

White, D. A. (2016b). The VIIRS Conversion Toolkit (MCTK) User's Guide. Available online: https://github.com/dawhite/VCTK/releases (accessed on 15 December 2016).

Xie, H. J., Wang, X. W., & Liang, T. G. (2009). Development and assessment of combined Terra and Aqua snow cover products in Colorado Plateau, USA and

northern Xinjiang, China. *Journal of Applied Remote Sensing*, *3*, 033559-033559.

Zhang, R., Huang, C., Zhan, X., Dai, Q., & Song, K. (2016). Development and validation of the global surface type data product from S-NPP VIIRS. *Remote Sensing Letters*, *7*, 51-60.